AD_____

Award Number: DAMD17-98-1-8034

TITLE: Role of TGF-1B1-Mediated Down Regulation of NF-kB/Rel
        Activity During Growth Arrest of Breast Cancer Cells

PRINCIPAL INVESTIGATOR: Shangqin Guo, Ph.D.
                         Gail E. Sonenshein, Ph.D.

CONTRACTING ORGANIZATION: Boston University
                           Boston, Massachusetts 02118

REPORT DATE: November 2002

TYPE OF REPORT: Annual Summary

PREPARED FOR: U.S. Army Medical Research and Materiel Command
               Fort Detrick, Maryland 21702-5012

DISTRIBUTION STATEMENT: Approved for Public Release;
                         Distribution Unlimited

The views, opinions and/or findings contained in this report are
those of the author(s) and should not be construed as an official
Department of the Army position, policy or decision unless so
designated by other documentation.

REPORT DOCUMENTATION PAGE

1. AGENCY USE ONLY (Leave blank)	2. REPORT DATE	3. REPORT TYPE AND DATES COVERED
	November 2002	Annual Summary (1 May 98 – 31 Oct 02)

4. TITLE AND SUBTITLE
Role of TGF-1B1-Mediated Down Regulation of NF-kB/Rel Activity During Growth Arrest of Breast Cancer Cells

5. FUNDING NUMBERS
DAMD17-98-1-8034

6. AUTHOR(S):
Shangqin Guo, Ph.D.
Gail E. Sonenshein, Ph.D.

7. PERFORMING ORGANIZATION NAME(S) AND ADDRESS(ES)

Boston University
Boston, Massachusetts 02118

E-MAIL: sqguo@bu.edu

8. PERFORMING ORGANIZATION REPORT NUMBER

9. SPONSORING / MONITORING AGENCY NAME(S) AND ADDRESS(ES)

U.S. Army Medical Research and Materiel Command
Fort Detrick, Maryland 21702-5012

10. SPONSORING / MONITORING AGENCY REPORT NUMBER

11. SUPPLEMENTARY NOTES
Original contains color plates: All DTIC reproductions will be in black and white.

12a. DISTRIBUTION / AVAILABILITY STATEMENT
Approved for Public Release; Distribution Unlimited

12b. DISTRIBUTION CODE

13. ABSTRACT *(Maximum 200 Words)*

see page 5

see page 5

14. SUBJECT TERMS
breast cancer, NF-kappaB, AhR, c-myc

15. NUMBER OF PAGES
31

16. PRICE CODE

17. SECURITY CLASSIFICATION OF REPORT	18. SECURITY CLASSIFICATION OF THIS PAGE	19. SECURITY CLASSIFICATION OF ABSTRACT	20. LIMITATION OF ABSTRACT
Unclassified	Unclassified	Unclassified	Unlimited

FOREWORD

Opinions, interpretations, conclusions and recommendations are those of the author and are not necessarily endorsed by the U.S. Army.

____ Where copyrighted material is quoted, permission has been obtained to use such material.

____ Where material from documents designated for limited distribution is quoted, permission has been obtained to use the material.

____ Citations of commercial organizations and trade names in this report do not constitute an official Department of Army endorsement or approval of the products or services of these organizations.

X In conducting research using animals, the investigator(s) adhered to the "Guide for the Care and Use of Laboratory Animals," prepared by the Committee on Care and use of Laboratory Animals of the Institute of Laboratory Resources, national Research Council (NIH Publication No. 86-23, Revised 1985).

X For the protection of human subjects, the investigator(s) adhered to policies of applicable Federal Law 45 CFR 46.

N/A In conducting research utilizing recombinant DNA technology, the investigator(s) adhered to current guidelines promulgated by the National Institutes of Health.

N/A In the conduct of research utilizing recombinant DNA, the investigator(s) adhered to the NIH Guidelines for Research Involving Recombinant DNA Molecules.

N/A In the conduct of research involving hazardous organisms, the investigator(s) adhered to the CDC-NIH Guide for Biosafety in Microbiological and Biomedical Laboratories.

Shange Grue 11/27/02
PI - Signature   Date

page 3

Table of Contents

Appendix: One paper

*Please note that the PI of this grant was changed from Dong Wook Kim to Shangqin Guo.

ABSTRACT

The NF-κB/Rel family of dimeric transcription factors has been shown to promote cell survival, and increasing evidence suggests involvement in carcinogenesis. Recently, NF-κB/Rel was found to be constitutively active in the nuclei of human breast cancer cell lines, as well as in 7,12-dimethylbenz(a)anthracene (DMBA)-induced mammary tumors from Sprague-Dawley (S-D) rats. Malignantly transformed human mammary epithelial cells (HMEC), derived by carcinogen treatment of non-tumorigenic parental MCF-10F cells, displayed increased constitutive NF-κB activation. In premalignant HMECs immortalized by carcinogen treatment *in vitro,* NF-κB activity was dysregulated in quiescence. To test the role of NF-κB in mammary tumorigenesis, we established founder lines of transgenic mice with targeted ectopic expression of the c-Rel subunit in the mammary gland. In the first cycle of pregnancy, the expression of transgenic c-*rel* mRNA was observed, and levels of c-Rel protein were increased in the mammary gland. Importantly, 31.6% of mice developed one or more mammary tumors at an average age of 19.9 months. Mammary tumors were of diverse histology and expressed increased levels of nuclear NF-κB. Analysis of the composition of NF-κB complexes in the tumors revealed aberrant nuclear expression of multiple subunits, including c-Rel, p50, RelA, RelB and the Bcl-3 protein, as observed previously in human primary breast cancers. In mammary carcinomas, as well as some grossly normal mammary glands from multiparous transgenic mice, expression of the cancer-related NF-κB target genes *cyclin D1,* and c-*myc* was significantly increased compared to mammary glands from wild-type mice or virgin transgenic mice. These results indicate for the first time that dysregulated expression of c-Rel, as observed in breast cancers, is capable of contributing to mammary tumorigenesis. Lastly, the effects of the green tea polyphenol epigallocatechin-3 gallate (EGCG) on Her-2/neu overexpressing breast cancer cells were examined. EGCG inhibited MMTV-Her-2/neu mouse mammary tumor NF639 cell growth in culture and soft agar. EGCG reduced signaling via the phosphatidylinositol 3-kinase, Akt kinase to NF-κB pathway due to inhibition of basal Her-2/neu receptor tyrosine phosphorylation. EGCG similarly inhibited basal receptor phosphorylation in the MMTV-Her-2/neu mouse mammary tumor SMF cells and in Ba/F3 2+4 cells, suggesting the potential beneficial use of EGCG in adjuvant therapy of tumors with Her-2/neu overexpression. Overall our studies provide evidence for involvement of the NF-κB/Rel in malignant progression of mammary epithelial cells.

Introduction

NF-κB/Rel is a family of transcription factors, which are expressed in all cells; however, in most non-B cells, they are sequestered in the cytoplasm in inactive complexes with specific inhibitory proteins, termed IκBs. We have recently shown that NF-κB/Rel factors are aberrantly activated in breast cancer, and function to promote tumor cell survival. Specifically, mammary tumors induced upon carcinogen treatment of Sprague-Dawley (S-D) rats, human breast tumor cell lines, and primary human breast tumor tissue samples were found to constitutively express high levels of nuclear NF-κB/Rel, whereas normal rat mammary glands and untransformed breast epithelial cells contained the expected low basal levels. Inhibition of this activity in breast cancer cells in culture via introduction of the specific inhibitory protein IκB-α led to apoptosis. Inhibition of breast cancer cell growth by TGF-β1 was shown to be mediated via decreased levels and activity of NF-κB. More recently we have performed a time course study of induction of NF-κB/Rel factors upon carcinogen treatment of female S-D rats, which revealed that NF-κB/Rel activation was an early event, occurring prior to malignant transformation. Furthermore, we have shown that transformation of MCF-10F untransformed human mammary epithelial cell (HMEC) line induced by the carcinogens 7,12-dimethylbenz(*a*)anthracene (DMBA) and benzo[*a*]pyrene (BaP) transformed (lines D3-1 and BP-1, respectively) results in activation of NF-κB/Rel subunits. Here the role of NF-κB in mammary tumorigenesis has been explored using a mouse model and cell culture studies.

II. Body

Progress Report

Technical Objectives 1 and 2:
1. Quantitate and characterize the NF-κB/Rel subunits induced in the DMBA and BaP transformed cell ines D3-1 and BP-1
2. Determine the kinetics of NF-κB/Rel induction in the PAH transformation process.

These two objectives have been completed, and the work published in Kim et al., 2000. A brief description of the work is as follows: We examined the time course of induction of NF-κB/Rel factors upon carcinogen treatment of female Sprague-Dawley (S-D) rats *in vivo* and in human mammary epithelial cells (HMECs) in culture. We observed that NF-κB/Rel activation is an early event, occurring prior to malignant transformation. In S-D rats, increased NF-κB/Rel binding was detected in nuclear extracts of mammary glands from 40% of animals 3 weeks post treatment with 15 mg/kg 7,12-dimethylbenz(*a*)anthracene (DMBA); this is prior to formation of tumors which normally begin to be detected after 7 to 9 weeks. In non-tumorigenic MCF-10F cells, *in vitro* malignant transformation upon treatment with either DMBA or benzo[*a*]pyrene (BaP) resulted in a 4- to 12-fold increase in activity of classical NF-κB (p65/p50). NF-κB induction was correlated with a decrease in the stability of the NF-κB specific inhibitory protein IκB-α. Ectopic expression of the transactivating p65 subunit of NF-κB in MCF-10F cells induced the c-*myc* oncogene promoter, which is driven by two NF-κB elements, and endogenous c-Myc levels. Furthermore, reduction mammoplasty-derived HMECs, immortalized following BaP exposure, showed dysregulated induction of classical NF-κB prior to malignant transformation. Together these findings suggest that activation of NF-κB plays an early, critical role in the carcinogen-driven transformation of mammary glands.

Technical Objective 3:
Use transgenic mice to study the contribution of c-Rel subunit expression in the development of breast neoplasia, including cross-breeding experiments with MMTV-TGF-β1 transgenic mice to define the role of TGF-β1 *in vivo*.

Generation and characterization of MMTV-c-*rel* transgenic mice. To determine the role of c-Rel in mammary tumorigenesis, we generated a mouse model where c-*rel* cDNA was expressed under the control of the MMTV-LTR promoter. Integration of the construct into the genome of potential founders was assessed by Southern blot analysis of tail DNA, and five founders successfully passed the transgene through the germline. Founder line 3 had approximately 3 copies of the transgene, while lines 7, 14, 15 and 18 had 4-5 copies and line 16 had approximately 9 copies, as estimated by comparison with bands resulting from hybridization with the endogenous gene on the Southern blots. MMTV-c-*rel* transgenic mice of all founders developed and bred normally. Transgenic females were able to nurse their pups.

To characterize the expression pattern of the c-*rel* transgene, line 14 MMTV-c-*rel* mice or wild-type (WT) FVB/N mice, as control, were bred to activate the MMTV-LTR promoter, which contains hormonally responsive elements activated by progestins and corticosteroids. At day 18.5 of the first pregnancy, total RNA was isolated from the mammary glands and various other organs. RNA samples were subjected to a radiolabeled transgene-specific RT-PCR assay, performed with a 5' mouse c-*rel* cDNA sense primer and a 3' SV40 poly(A) antisense primer.

7

Expression of c-*rel* transgene mRNA was observed in the mammary gland of line 14, but not the WT mouse, as expected (Fig. 1A, left panel). RNA quality and equal loading was confirmed by analysis of β-actin mRNA expression profiles by RT-PCR (Fig. 1A, bottom panel), as well as by ethidium bromide-stained gels (data not shown). At day 18.5 of pregnancy, expression of transgene c-*rel* mRNA was also observed in the spleen, salivary gland, and intestine of mice from line 14 (Fig. 1A) and line 16 (data not shown), while undetectable or low levels were observed in the kidney and liver (Fig. 1A) and heart and lung (data not shown). Where indicated, reactions were performed in the absence of reverse transcriptase (RT), which confirmed the absence of DNA contamination. Thus, the c-*rel* transgene mRNA is expressed mostly in glandular organs and lymphoid tissues, which is consistent with previous studies with the MMTV-LTR promoter.

We next sought to determine total levels of c-Rel protein expression, which includes both endogenous and transgenic c-Rel. At day 18.5 of the first pregnancy, nuclear extracts were prepared from mammary glands of transgenic lines 7, 14, 15, 16 and 18 mice, and from a WT FVB/N mouse as control. Samples were subjected to immunoblot analysis for c-Rel and Sp1 to normalize for loading (Fig. 1B). Nuclei from the WT mammary gland contained basal levels of c-Rel, as has been reported recently. All of the transgenic lines displayed higher normalized levels of nuclear c-Rel. The lowest level was seen in line 18, consistent with its low transgene copy number, as seen above; therefore, the other four lines (i.e. lines 7, 14, 15 and 16) were chosen for further study.

MMTV-c-*rel* transgenic mice develop late-onset mammary carcinomas. To promote c-*rel* transgene overexpression, MMTV-c-*rel* female mice were continuously bred to induce the MMTV-LTR promoter. A cohort of 38 multiparous female mice from the 4 expressing lines was monitored for tumor incidence over 2 years. Mice were subjected to bi-weekly palpable examination, and when the presence of a tumor was detected, the mammary glands and other organs were subjected to histopathological analysis. 31% of the mice developed mammary carcinomas at an average age of 19.9 months (Table 1). In contrast, mammary tumors develop with a very low incidence (<1%) in WT female FVB/N mice that have been similarly bred. An identification number, with the origin of the line was attributed to each tumor, and characteristics of the different breast tumors are described in the Table 1. Mice from each of the four transgenic lines developed mammary carcinomas. The tumor incidence was 33.3, 41.7, 20 and 33.3% in MMTV-c-*rel* transgenic lines 7, 14, 15 and 16, respectively (data not shown), suggesting that tumor development is related to c-*rel* transgene expression rather than random insertional events. In all but one case, the tumors arose as solitary masses in a single mammary gland. Of the 12 mammary tumors, 3 were pure adenocarcinomas (Fig. 2A), 3 were adenosquamous carcinomas (Fig. 2C), 4 were squamous cell carcinomas (Fig. 2D), 1 was classified as a papillary adenocarcinoma, and 1 was a spindle cell carcinoma (Fig. 2E). Spindle cell carcinomas are often related to an epithelial to mesenchymal cell transition (EMT), which is the transformation of epithelial cells into cells with features of mesenchymal cells, favoring the progression of a carcinoma towards a dedifferentiated and more malignant state. To test for cells of epithelial origin, immunohistological staining was carried out using antibodies specific for the epithelial cell marker cytokeratin 8 (Fig. 2F). The spindle cell carcinoma stained positively for cytokeratin 8, consistent with an EMT tumor. One of the adenocarcinomas was metastatic to the lung (Fig. 2B).

Lastly, mammary glands of 3 other multiparous 2 years-old transgenic mice, that were not included in the cohort, were subjected to histopathological analysis even without the

presence of a palpable tumor. This examination revealed the presence of an adenosquamous carcinoma and a mammary squamous cell carcinoma in 2 of the mice (data not shown). In addition to the tumors, poor regression of the alveolar tree of the mammary gland after pregnancy was another histological abnormality that was frequently seen (Table 1 and data not shown). Therefore, the histology of mammary tumors in MMTV-c-*rel* mice appears variable, suggesting changes in mammary epithelial cells during c-Rel-induced tumorigenesis.

c-Rel expression is elevated in mammary glands and tumors of MMTV-c-*rel* transgenic mice. Previous studies showed that the MMTV-LTR promoter is still active in regressing mammary glands, leading to sustained transgene expression over the animal's lifetime. We therefore investigated transgenic c-*rel* expression in mammary glands and tumors from multiparous transgenic mice. RNA was isolated from mammary tumors of mice from transgenic lines 14 and 16 and from grossly normal mammary glands from age-matched transgenic mice (16-24 months) that had bred at least three times. In addition, RNA was isolated from mammary glands of a nulliparous (virgin) WT FVB/N mouse and a virgin transgenic line 16 female as negative controls. Samples were subjected to a radiolabeled transgene-specific RT-PCR assay (Fig. 3A). As a control for DNA contamination, reactions were performed in the presence or absence of RT. RNA quality and essentially equal loading was confirmed by analysis of β-*actin* mRNA expression profiles by RT-PCR (Fig. 3A, bottom panel), and by ethidium bromide staining of the gels (data not shown). All tumors and most normal mammary glands of multiparous MMTV-c-*rel* transgenic mice exhibited expression of transgene mRNA, although at variable levels (Fig. 3A, top panel). In tumors, the lowest expression level of transgene mRNA was observed in the mammary tumor developed in mouse 4521 (line 16), whose histologic analysis showed a complex cell pattern, consisting of mammary squamous cell carcinoma and hyperplasic epithelial cells (Table 1). In contrast, virgin WT and transgenic mammary glands did not express detectable levels of transgene mRNA, as expected. Thus, ectopic c-*rel* transgene expression is induced in the mammary gland by pregnancy, and is expressed in the tumors and grossly normal mammary glands of multiparous MMTV-c-*rel* mice.

We next assessed total c-Rel protein expression in mammary glands and tumors of transgenic mice by immunoblot analysis. Nuclear extracts were prepared from the indicated tumors (Fig. 3B). As a control, nuclear extracts were isolated from mammary glands of a WT virgin FVB/N mouse and from non-malignant mammary glands of an age-related line 14 mouse (3000 N), that had undergone 3 cycles of pregnancy and regression. The mammary gland of the line 14 mouse (3000 N) and all tumors displayed elevated levels of c-Rel expression compared to the WT mammary gland, which showed only a low basal expression (Fig. 3B and data not shown). This is consistent with the pattern of transgenic c-*rel* expression obtained above. In addition, about half of the tumors showed higher expression levels of c-Rel than grossly normal transgenic mammary glands (Fig. 3B and data not shown). When the results were scanned, a 3 to 150 (average 68.0 ± 60.1)-fold increase in nuclear c-Rel expression was observed in tumor and normal transgenic mammary glands as compared to the WT sample. Equal loading was confirmed by Coomassie blue staining of the gels (Fig. 3B, bottom panel); although, the patterns of total protein expression appeared different between tumor samples and WT or normal transgenic mammary gland samples. This variability likely results from differences in cell type composition between the various mammary tumors and the normal tissue. Overall, these results indicated that c-*rel* transgenic mRNA and total c-Rel protein expression are upregulated in MMTV-c-*rel* mammary glands and tumors as compared to WT mice.

Expression of NF-κB family members in mammary glands and carcinomas of MMTV-c-*rel* transgenic mice. To test for constitutive nuclear c-Rel binding activity, nuclear proteins were isolated from a mammary tumor (adenocarcinoma) and grossly normal mammary glands of line 15 mouse 127, and subjected to EMSA analysis with an oligonucleotide probe containing the NF-κB element upstream of the c-*myc* promoter, which binds all Rel family members (Fig. 4A). The normal mammary gland displayed a low level of NF-κB binding (better seen on a darker exposure), consistent with our previous findings with nuclear extracts from normal rat mammary glands and histologically normal mammary tissue from MMTV-Her-2/neu transgenic mice. The extracts from the c-Rel-induced tumor displayed two major complexes of NF-κB binding. To identify the nature of the subunit components, we used antibodies against either c-Rel or p50 in EMSA. Addition of an antibody that preferentially recognizes p50 in a homodimer complex, shifted the bottom band completely, and reduced the more slowly migrating complex. Addition of a blocking antibody against c-Rel selectively reduced the top band. These results suggest that the upper complex consisted of p50/c-Rel heterodimers, while the bottom complex was a homodimer of p50.

We next performed EMSA on a second mammary tumor (adenocarcinoma) sample from line 14 (3996) mouse. This mouse had developed 4 mammary adenocarcinomas, as well as pulmonary metastases (see Table 1 above). Nuclear extracts isolated from one of the 4 mammary tumors (3996R1) displayed multiple NF-κB complexes (Fig. 4B). The level of NF-κB binding was more intense than seen with the nuclear extract from a non-malignant mammary gland from the same animal (line14 3996 N), while levels of control Oct-1 binding were similar in these samples (Fig. 4C). Of note, an NF-κB complex of faster mobility was present in the normal sample. We previously observed the presence of such a complex in nuclear extracts isolated from normal human and mouse breast tissue, and supershift analysis showed that these complexes contained predominantly p50 homodimers (data not shown). Addition of supershifting antibodies against p50, c-Rel, RelA, or RelB, resulted in shifted complexes with the line 14 3996R1 extracts. In particular, addition of a p50 antibody greatly reduced binding and yielded two major and a few minor supershifted bands. Addition of a c-Rel-specific antibody resulted in diminished binding and the formation of one slower migrating supershifted complex (Fig. 4B, indicated by an arrowhead). As a control for the EMSA, a similar analysis was performed with a nuclear extract from WEHI 231 immature B lymphoma cells, which express high levels of activated c-Rel and p50, and low levels of RelA. Addition of an antibody against c-Rel reduced the binding and yielded a similar supershifted complex with WEHI 231 extracts, indicating that the line14 3996R1 tumor sample contains p50/c-Rel complexes. Interestingly, addition of a RelA antibody yielded three supershifted RelA-containing complexes with the tumor sample, and the one-RelA-containing complex (e.g. p50/RelA) with the WEHI 231 extract. These results suggest that RelA is present in multiple complexes in the mammary gland tumor sample. Lastly, a RelB antibody also reduced binding with the line 14 tumor extract, yielding one supershifted complex (Fig 4B). Addition of the RelB antibody had no detectable effect on the WEHI 231 cells as expected, consistent with the lack of nuclear RelB in these cells. Together, these results indicate that multiple NF-κB subunits are activated in this tumor sample, including p50, c-Rel, RelA, and RelB.

Mammary tumors contain multiple NF-κB subunits. The finding that nuclear extracts of mammary tumors from the MMTV-c-*rel* mice contain multiple NF-κB complexes led us to more fully assess the nature of the NF-κB subunit expression in mammary glands and tumors. Immunoblot analysis was performed for the p50, RelA, RelB, and p52 NF-κB subunits, and for

Bcl-3 protein in nuclear extracts from mammary tumors developed in MMTV-c-*rel* mice, and from uninvoluted mammary glands from a multiparous age-matched line 14 transgenic mouse (3000 N), and from a WT virgin FVB/N mouse (Fig. 5). Interestingly, expression of the subunits encoded by genes that are regulated by NF-κB, e.g. p50, p52 and RelB, appeared substantially increased in many of the samples from the transgenic mice. A dramatic increase in expression of p50 was seen in essentially all of the tumor specimens, as well as grossly normal transgenic mammary gland samples compared to the WT sample. Densitometry indicated a 2.1 to 618 (average 330 ± 325)- fold induction in p50 nuclear levels. Expression of RelB displayed a large increase in 3 of the specimens compared to the WT mammary gland sample, and a moderate increase in the other 4 samples. In contrast, RelA appeared only moderately increased in most transgenic mammary glands compared to WT mammary glands. Densitometry showed a 1.0 to 1.6 (average 1.3 ± 0.4)-fold increase in RelA nuclear expression. Interestingly, this contrasted with the relatively high level of RelA binding previously seen in the EMSA of line 14 3996R1 (Fig. 4B), and of other 2 tumor samples that were similarly analyzed (data not shown). Bcl-3 expression was detectable only in tumor samples, and two of them also displayed extremely high levels of p50 and p52 expression. Overall, these findings indicate that in addition to the c-Rel subunit itself, the MMTV-c-*rel* mammary gland tumors display a wide range of constitutively active nuclear NF-κB subunits, including p50, p52, and RelB, and to a lesser extent RelA, as well as Bcl-3. Similar complex patterns were seen previously in primary human breast cancer specimens.

MMTV-c-*rel* mammary glands and carcinomas display elevated expression of downstream target gene *cyclin D1*. The NF-κB target gene *cyclin D1* has been implicated in breast cancer formation. Its expression, which is upregulated in ~50% of human breast tumors, is required for proliferation of breast cancer cells in culture, and MMTV-*cyclin D1* mice develop mammary adenocarcinomas. Therefore, we sought to test whether *cyclin D1* mRNA levels were increased during pregnancy in the mammary glands of MMTV-c-*rel* *vs* WT mice. Lines 7, 15 and 16 MMTV-c-*rel* mice and age-matched WT FVB/N mice (3 to 6 month-old) were bred to activate the MMTV-LTR promoter in transgenic mammary glands. At day 18.5 of the first pregnancy, total RNA was isolated from the mammary glands and samples subjected to a semi-quantitative RT-PCR assay specific for *cyclin D1* in the presence, or absence of RT as control for DNA contamination (Fig. 6A). RNA quality and loading were normalized by evaluation of β-*actin* levels by RT-PCR using 25 cycles of PCR, which is within the linear phase of amplification. The level of *cyclin D1* mRNA was higher in all of transgenic mouse mammary glands compared with the three WT mouse samples. When results of this and a duplicate experiment were scanned and normalized to β-*actin* mRNA levels, a 2.5 ± 0.8-fold increase ($P < 0.003$) in *cyclin D1* mRNA levels were observed in transgenic samples. Thus, overexpression of transgenic c-Rel in the mammary gland during the first pregnancy is sufficient to induce a significant increase in *cyclin D1* mRNA expression.

We next evaluated *cyclin D1* levels in c-Rel-induced mammary tumors compared to non-malignant mammary glands in transgenic animals. Total RNA was isolated from 4 mammary carcinomas that had developed in transgenic mice of lines 14 and 16, as well as from 2 grossly normal mammary glands from multiparous age-matched transgenic mice from the same lines. Samples were subjected to semi-quantitative RT-PCR for *cyclin D1* mRNA expression (Fig. 6B). In this and a duplicate experiment, all of the tumors displayed higher expression levels of *cyclin D1* as compared to the two grossly normal mammary gland samples tested. Interestingly, the normal sample 14 (5441 N) displayed higher levels of *cyclin D1* mRNA than the normal sample

16 (4948 N), which correlated with their respective levels of c-*rel* transgene expression as seen above (Fig. 3A). Therefore, MMTV-c-*rel* mammary glands and carcinomas display a substantial overexpression of *cyclin D1* mRNA as compared to the WT mammary gland.

Evidence has also suggested NF-κB mediates regulation of *cyclin A*. Thus, we compared the overall cyclin expression profiles in the c-Rel-induced mammary tumors with the grossly normal mammary glands. In the first set, total RNA was prepared from two grossly normal mammary glands of multiparous transgenic mice from line 14 (4949 N and 4946 N), and two mammary tumors from line 14 (3814 T) and 16 (4528 T). In a second set, total RNA was prepared from mammary carcinomas of line 14 (4936 T and 4556 T) and line 16 (4521 T). RNA samples were subjected to a multi-probe RNAase Protection Assay (RPA) kit, which assesses mRNA levels for *cyclins A1, A2, B1, B2, C, D1, D2,* and *D3,* and *L32* and *GAPDH* housekeeping gene products (Fig. 7). In this and a duplicate experiment, bands were detectable for *cyclin A2, B1, D1, D2* and *D3* mRNA. The mRNA from the c-Rel-induced tumors displayed increased expression of the *cyclin D1* gene as compared to the normal mammary glands (Fig. 7, left panel), consistent with the RT-PCR analysis above (Fig. 6B). The tumors displayed variable levels of mRNA for *cyclins A2, B1, D2* and *D3*. Analysis of the housekeeping genes L_{32} and *GAPDH* confirmed essentially equal loading of samples within the panels. Thus, RPA showed that MMTV-c-*rel* tumors display an increase in *cyclin D1* gene expression with variable expression level of the other cyclins.

MMTV-c-*rel* mammary tumors overexpress c-*myc*. We next tested for changes in c-*myc* gene expression, another NF-κB target gene, which affects cell proliferation and survival. RNA was isolated at day 18.5 of the first pregnancy from mammary glands of line 7, 15 and 16 MMTV-c-*rel* transgenic and WT FVB/N mice, all aged 3 to 6-months. Samples were subjected to Northern blot analysis for c-*myc* RNA levels (Fig. 8A). The quality of the RNA was evaluated by ethidium bromide staining of the gel (Fig. 8A) and by Northern blot analysis for *GAPDH* mRNA expression (data not shown). The level of c-*myc* mRNA appeared to be higher in most of the mammary glands from the transgenic animals as compared to those from the two WT mice. When results were scanned and normalized to 28S rRNA levels, a 2.4 ± 1.4-fold increase was observed in c-*myc* mRNA expression levels in transgenic samples as compared to the average of the WT samples. Comparable increase was obtained upon normalization to levels of *GAPDH* mRNA (2.8 ± 0.7-fold, data not shown). These levels of increase did not reach statistical significance.

We next compared the c-*myc* mRNA expression levels in normal mammary glands *vs* carcinomas developed from multiparous age-matched transgenic mice, as well as a virgin transgenic mouse. Quality of the RNA and equal loading was controlled by ethidium bromide staining of the gel (Fig. 8B) and by RT-PCR analysis of β-actin mRNA levels, as shown above in Figure 6 (bottom panel). In Northern blot analysis, all the c-Rel-expressing samples from multiparous transgenic mice, either normal mammary glans or tumor, demonstrated a substantial increase in c-*myc* mRNA expression levels as compared to the virgin mouse sample from line 16. When the results were scanned and normalized to 28S rRNA levels, a 16.5 ± 8.3-fold increase in c-*myc* mRNA expression levels was observed in mammary glands of multiparous transgenic mice compared to the virgin transgenic mouse sample. In addition, tumors displayed a 2.3 ± 0.8-fold increase in levels of c-*myc* RNA expression as compared to grossly normal mammary glands of multiparous MMTV-c-*rel* transgenic mice (*P* < 0.028) (Fig. 8B). Thus, increased c-*rel* expression in trangenic mice led to elevated levels of c-*myc* mRNA in mammary glands and carcinomas.

Overall, these findings demonstrate for the first time that c-Rel plays a causal role in tumorigenesis of the mammary gland in an MMTV-LTR-driven mouse model. Overall, one or more mammary tumors were detected in 31.6% of MMTV-c-*rel* transgenic mice at an average age of 19.9 months. Histological analysis of the mammary tumors in 4 independent lines provided evidence for a wide spectrum of tumor subtypes, including adenocarcinomas, adenosquamous carcinomas, squamous carcinomas, a spindle cell carcinoma and a papillary carcinoma. One mouse developed pulmonary metastasis in addition to multiple mammary adenocarcinomas. In addition to mammary carcinomas, several mice had enlarged spleen or other abnormalities including lymphoid or myeloid hyperplasia or centrolytic lymphomas in the spleen, which can be correlated to the expression of the transgene in splenocytes (Fig. 1A), and as also shown in previous studies with transgenic mice using the same promoter. By contrast, only rare (<1%) spontaneous cases of mammary tumors were reported in the FVB/N strain, consisting of squamous carcinomas or ketatoacanthomas. The MMTV-c-*rel* mammary tumors displayed sustained expression of the c-*rel* transgene mRNA. Tumors were also typified by overexpression of c-Rel protein, and displayed elevated mRNA levels of *cyclin D1*, and c-*myc*, NF-κB target genes implicated in growth control. These changes were detected in normal mammary glands during and after the first cycle of pregnancy. While the v-*rel* oncogene, the viral homologue of c-Rel, has been shown to be highly tumorigenic, our findings represent the first *in vivo* demonstration of the transforming ability of the c-Rel NF-κB subunit.

While it was originally proposed to cross the MMTV-c-Rel mouse with an MMTV-TGF-β1 mouse to see if this will delay or ablate tumor formation, the late onset of tumor appearance essentially precluded these studies. Hence I proposed to alter the objective to see if crossing our mice with an MMTV-CK2 mouse can enhance the rate of tumor formation. The rationale for this change in proposed work is that we have recently shown that ectopic protein kinase CK2 (formerly known as casein kinase II) activity can increase NF-κB expression and activity in breast cancer cell lines, and in mouse mammary tumors (Romieu-Mourez et al., 2001; Landesman-Bollag et al., 2001). Furthermore, we have shown that CK2 levels are elevated in primary human breast cancer specimens (Romieu-Mourez et al., 2001). Thus, I proposed to test the hypothesis that the latency of tumor appearance in the MMTV-c-Rel/CK2 bitransgenic mice will be shorter than in the single transgenic mice (approximate median age 19.9 and 23 months, respectively). I have now bred the animals and am currently in the process of assessing tumor appearance.

Technical Objectives 4 and 5:
4. Investigate the effects of TGF-β1 on NF-κB/Rel activity in the PAH transformed cell lines.
5. Study the cooperative effect of TGF-β1 and chemotherapeutic drugs on cell lines.

As discussed above, the experiments on the TGF-β1/c-Rel bitransgenic mice no longer appear feasible. Thus, I have begun examining the role of other inhibitors of NF-κB. Recent work by several groups have indicated that polyphenols in green tea extracts can inhibit induction of NF-κB. Using the MMTV-Her-2/neu tumor cells, termed NF639, which we have recently shown expressed constitutive NF-κB (Pianetti et al., 2001), we examined the effects of the most abundant polyphenol in green tea extracts, epigallocatechin-3 gallate (EGCG) (Kavanagh et al., 2001).

EGCG Inhibits Growth of MMTV-Her-2/neu Breast Cancer Cell Lines. We first tested the ability of EGCG to inhibit growth of the MMTV-Her-2/neu mouse breast tumor derived cell line NF639. Cultures were plated, in triplicate, at a density of 3.9×10^3 cells/cm^2. After 24 h, EGCG was added to a final concentration of 20-160 μg/ml or the volume of carrier DMSO equivalent to the highest dose was added. Cell growth was assessed every 24 hours using a non-radioactive MTS cell proliferation assay (Fig 9). A dose-dependent decrease in the rate of proliferation was seen with 20 and 40 μg/ml EGCG, whereas, no cell growth was seen with 80 μg/ml EGCG. Upon treatment with 160 μg/ml EGCG, a drop in cell numbers was seen. This suggested that extensive death of NF639 cells was occurring only at this higher dose, which was confirmed by trypan blue staining of cells with 0, 40, 80 or 160 μg/ml EGCG (data not shown). Thus, treatment of the NF639 breast tumor cells with 20-80 μg/ml EGCG decreases their rate of proliferation in culture.

EGCG Inhibits Growth of NF639 Cells in Soft Agar. Growth in soft agar is a hallmark of transformed phenotype. Hence, we next assessed the ability of EGCG to reduce growth of NF639 cells in soft agar. NF639 cells were plated, in triplicate, at a density of 7.5×10^3 cells/ml in top plugs consisting of complete medium and 0.8% SeaPlaque agarose containing 0, 20, 40 or 80 μg/ml EGCG. The plates were incubated for two weeks and colonies stained with crystal violet and counted as described in the figure legend to Fig 10. A decrease in colony numbers was seen which was more pronounced with increasing doses of EGCG (Fig. 10, inset). Quantitation of the results confirmed inhibition of colony formation occurred in a dose-dependent fashion with EGCG treatment (Fig. 10). Thus, EGCG inhibits growth in soft agar, an important property of the transformed phenotype.

EGCG Reduces NF-κB Activity in the NF639 Cell Line. To assess the effects of EGCG on Her-2/neu signaling, we first monitored the recently identified downstream target NF-κB. NF639 cells were treated with 40 μg/ml EGCG for 24 h and nuclear extracts prepared. These were used in EMSA with an oligonucleotide containing the NF-κB element upstream of the c-*myc* promoter. Extracts from DMSO-treated cells gave rise to two bands (Fig. 11A). These have been identified previously as containing complexes composed of p65/p50 and p50 homodimers (p50/p50). Incubation in the presence of 40 μg/ml EGCG reduced formation of both of these two complexes. This decrease was selective, as no change was seen in Sp-1 binding (Fig. 11A). We next assessed the effects of EGCG on NF-κB activity. A transfection assay was performed using an NF-κB element-driven luciferase reporter. In two experiments, treatment with 50 μg/ml EGCG for 24 h reduced NF-κB activity by 76.3% +/- 5.9%. Thus, EGCG inhibits NF-κB binding and activity in NF639 cells.

EGCG Inhibits the PI 3-Kinase to Akt Kinase Signaling Pathway. Previously, we showed that induction of NF-κB in NF639 cells occurs via a PI 3-kinase to Akt kinase pathway. To test the effect of EGCG treatment on Akt phosphorylation the cells were incubated for 24 h in the presence of either 40 μg/ml of EGCG that had been dissolved in DMSO, or the equivalent amount of carrier solution. Alternatively, cells were incubated in the presence of 100 nM Wortmannin, a potent specific inhibitor of PI 3-kinase. Whole cell extracts (WCEs) were prepared and immunoprecipitated with a monoclonal antibody against Akt, which preferentially recognizes phosphorylated protein. GSK3α-GST was then used as the substrate for the resulting immunoprecipitated Akt, and the phosphorylated material identified by immunoblot analysis for phosphorylated GSK3α -GST protein (Fig. 11B). The EGCG treatment resulted in a dramatic

decrease in phosphorylated GSK3α -GST. A similar decrease was observed with Wortmannin treatment.

As a test for the effects of EGCG on PI 3-kinase activity, we measured the presence of phosphorylated Akt, which is one of its critical signaling substrates. Immunoblotting was performed using an antibody specific for phospho-Akt (Ser473). Treatment with EGCG caused an ~50% decrease in phosphorylated Akt protein (Fig. 11C). A similar level of decrease was observed upon treatment with Wortmannin, suggesting the remaining phosphoprotein detected is due to other kinase activities. Immunoblotting for β-actin confirmed equal loading. Together, these results demonstrate the ability of EGCG to reduce the activities of both PI 3-kinase and Akt.

EGCG Reduces Basal Phosphorylation of Her-2/neu. Overexpression of Her-2/neu can lead to constitutive phosphorylation and basal receptor activation and signaling. Thus, we tested whether treatment with EGCG can reduce this basal Her-2/neu phosphorylation. NF639 cells were treated with 0, 20, 40 or 80 μg/ml EGCG for 48 h. WCEs were isolated and subjected to immunoblot analysis using a tyrosine phosphospecific Her-2/neu antibody (Fig. 12A). A dose-dependent drop in phosphorylated Her-2/neu protein was noted. Densitometry indicated treatment with 20, 40 or 80 μg/ml caused a decrease of 13, 38, and 96%, respectively compared to control cells. Immunoblotting for β-actin confirmed equal loading. To verify that this effect was general, we analyzed two additional cell lines: 1) SMF cells, similarly derived from an MMTV-Her-2/neu mouse mammary tumor; 2) Ba/F3 2+4 cells, a pro-B cell line clone stably expressing Her-2/neu + EGFR-4, displaying high constitutive Her-2/neu activity. SMF and Ba/F3 2+4 cells were treated with 40 μg/ml EGCG for 24 h and analyzed by immunoblotting for phosphorylated Her-2/neu (Fig. 12B). EGCG treatment similarly reduced basal phosphorylation of Her-2/neu in both cell lines. Thus, EGCG reduces the basal phosphorylation and constitutive activation of the Her-2/neu receptor. A copy of this paper is enclosed.

Overall, these studies show that the green tea polyphenol EGCG inhibits the signaling by Her-2/neu that promotes cell proliferation, survival and transformed phenotype. Treatment of MMTV-Her-2/neu mammary gland tumor NF639 cells with doses of EGCG up to 80 μg/ml slowed growth and dramatically reduced colony formation in soft agar with little effect on cell viability. Higher doses (160 μg/ml) reduced cell numbers and induced cell death as judged by trypan blue assays. Previously, we demonstrated that the overexpression of Her-2/neu in NF639 cells leads to the induction of NF-κB via a PI 3-kinase/Akt kinase signaling pathway. (Pienetti et al. 2001) EGCG inhibited this Her-2/neu signaling as judged by the observed decreases in PI 3-kinase, Akt kinase, and NF-κB activities. Furthermore, EGCG inhibited constitutive Her-2/neu phosphorylation in NF639 cells, as well as in SMF cells, a second MMTV-Her-2/neu mouse tumor-derived cell line, and Ba/F3 2+4 cells, a pro-B cell line transfected to express Her-2/neu + EGFR-4. Overall, these studies demonstrate for the first time that EGCG can ablate the Her-2/neu signaling cascade in breast cancer cells, by reducing basal Her-2/neu receptor phosphorylation. These results suggest further study of the potential role of EGCG in adjuvant therapy treatment modalities and of green tea components in chemoprevention of breast cancer are warranted.

Cited Literature

Kim, D.W., L. Gazourian, S.A. Quadri, R. Romieu-Mourez, D.H. Sherr, and G.E. Sonenshein. The RelA NF-κB subunit and the Aryl Hydrocarbon Receptor (AhR) cooperate to transactivate the c-*myc* promoter. Oncogene 19, 5498-5506 (2000).

Pianetti, S., M. Arsura, R. Romieu-Mourez, R.J. Coffey, and G.E. Sonenshein. Her-2/neu overexpression induces NF-κB via a PI3-kinase/Akt pathway without IKK activation that can be inhibited by the tumor suppressor PTEN. Oncogene 20, 1287-1299 (2001).

Landesman-Bollag, E., R. Romieu-Mourez, D.H. Song, G.E. Sonenshein, R.D. Cardiff, and D.C. Seldin. Protein kinase CK2 in mammary gland tumorigenesis. Oncogene 20, 3247-3257 (2001).

Romieu-Mourez, R., E. Landesman-Bollag, D.C. Seldin, A.M. Traish, F. Mercurio, and G.E. Sonenshein. Roles of protein kinase CK2 and IKK kinases in activation of NF-κB in breast cancer. Cancer Res. 61, 3810-3818(2001).

Kavanagh, K.T., L.J. Hafer, D.W. Kim, K.K. Mann, D.H. Sherr, A.E. Rogers, and G.E. Sonenshein. Green tea extracts decrease carcinogen-induced mammary tumor burden in rats and rate of breast cancer cell proliferation in culture. J. Cell Biochem. 82, 387-398 (2001).

III. Figure legends:

FIG. 1. MMTV-LTR-driven c-*rel* transgene expression in FVB/N mice. A) Transgenic c-*rel* expression. Total RNA was isolated from the indicated tissues of WT FVB/N or line14 MMTV-c-*rel* mice at day 18.5 of the first pregnancy, and subjected to DNAse treatment. Subsequently the samples (5 μg) were subjected to RT-PCR analysis, in the presence or absence of reverse transcriptase (+/- RT) to control for DNA contamination, using c-*rel* transgene-specific primers, amplifying a 236 bp fragment. Similar analysis of β-*actin* RNA levels confirmed the integrity of the reverse transcription reaction. B) Total c-Rel expression. Mammary glands were removed from WT FVB/N or the transgenic mice from independent founder lines as indicated at day 18.5 of the first pregnancy. Nuclear extracts were prepared, and samples (20 μg) subjected to immunoblot analysis of c-Rel, and Sp1, as control for loading. As additional controls, nuclear and whole cell extracts from the WEHI 231 immature B lymphoma cells, which expresses high constitutive levels of c-Rel were similarly analyzed. The values of c-Rel normalized to Sp1 level relative to the WT sample are displayed below.

FIG. 2. Representative histopathologies of mammary tumors that develop in MMTV-c-*rel* transgenic mice after multiple cycles of pregnancy and regression. A) Adenocarcinoma; B) Pulmonary metastasis in a mouse with mammary adenocarcinomas; C) Adenosquamous carcinoma showing areas with extracellular squamous differentiation (arrow); D) Squamous cell carcinoma; E) Spindle cell carcinoma; F) Immunohistochemistry for cytokeratin 8 expression in the spindle cell carcinoma shown in 2E; Note the staining of many of the spindle cells and staining of luminal epithelium in the glands (arrow).

FIG. 3. Expression of c-Rel in breast tumors developed in MMTV-c-*rel* transgenic mice. Mammary glands were removed from virgin WT FVB/N (WT Virgin) or transgenic line16 (16

Virgin) mice, tumor (T) and grossly normal (N) tissues of multiparous line 14 and 16 transgenic mice. The identification number given to the individual mice is indicated in parenthesis. Characteristics of the tumor samples are given in the Table 1. A) Transgenic c-*rel* expression. RNA was prepared from normal mammary gland and tumor tissues, and samples subjected to RT-PCR with primers specific for transgenic c-*rel*, as in the legend to Figure 1. B) Total c-Rel protein expression. Nuclear extracts were prepared, and samples (40 µg) subjected to immunoblot analysis for c-Rel. Coomassie-blue staining of SDS-PAGE gels was used as control for equal loading (bottom panel). While the overall levels of staining were essentially equivalent, the analysis revealed that the patterns of protein expression are different between tumors, WT and normal transgenic mammary gland samples. This variability likely results from differences in cell type composition in these tissues.

FIG. 4. MMTV-c-*rel* tumors display elevated NF-κB binding. A) Nuclear extracts were prepared from MMTV-c-*rel* line 15 (127) mouse mammary tumor and grossly normal mammary glands, and samples (5 µg) subjected to EMSA for NF-κB binding. To identify subunit composition, the indicated samples were incubated overnight at 4^0C in the absence (-) or presence of a supershifting antibody specific for p50, or a blocking antibody specific for c-Rel. The positions of the identified p50/c-Rel and p50 homodimer complexes are as indicated. B and C) Nuclear extracts were prepared from line 14 mammary tumor (3996R1 T) and grossly normal mammary glands (N), and samples (5 µg) subjected to EMSA for NF-κB (B) and Oct-1 (C), as loading control. For supershift analysis, samples were incubated overnight at 4^0C in the absence (-) or presence of supershifting antibodies specific for p50, RelA, c-Rel and RelB. The arrow shows the position of the supershifted c-Rel complex. Where indicated, nuclear extracts (5 µg) of WEHI 231 B cells, which express high levels of c-Rel/p50 complexes, were analyzed as a positive control in the same experiment, however a lighter exposure is shown for the WEHI 231 samples.

FIG. 5. MMTV-c-*rel* tumors express multiple NF-κB subunits and the Bcl-3 protein. Nuclear extracts were prepared from the indicated mammary tumors, grossly normal mammary glands (N) of multiparous line 14 MMTV-c-*rel* mice, and from mammary glands of a WT nulliparous FVB/N mouse (WT Virgin). Samples (40 µg) were subjected to immunoblot analysis for p50, RelA, RelB, and p52 NF-κB subunits and the Bcl-3 protein. As a control for equal loading, the gel was stained with Coomassie-blue, as discussed in the legend of Figure 3. The positions of molecular weight markers are as indicated (in kDa).

FIG. 6. MMTV-c-*rel* mammary glands and carcinomas overexpress *cyclin D1* mRNA. A) Mammary glands. Total RNA was prepared from mammary glands of 3 to 6 months-old transgenic mice or WT FVB/N mice at day 18.5 of the first pregnancy. RNA was subjected to DNase treatment, and analysis by ethidium bromide stained gels verified RNA quality and essentially equal loading (data not shown). Samples (5 µg) were subjected to RT-PCR analysis of *cyclin D1* and β-*actin* mRNA levels in the presence (+) or absence (-) of RT to control for DNA contamination. For the β-*actin* mRNA analysis, 25 PCR cycles was selected for normalization. The values of *cyclin D1* signal intensity normalized to β-*actin* mRNA levels are presented relative to the WT (3) sample. B) Mammary carcinomas. Total RNA was prepared from the indicated mammary tumors (T) and grossly normal mammary glands (N) of age-matched multiparous line 14 and 16 MMTV-c-*rel* mice. RNA samples (5 µg) were subjected to

17

semi-quantitative RT-PCR analysis to assess *cyclin D1* mRNA levels, as described above. The values of *cyclin D1* signal intensity normalized to β-*actin* RNA levels are presented relative to the line 16 (4948 N) normal sample (which was better seen on a darker exposure).

FIG. 7. Profile of cyclin gene expression in MMTV-c-*rel* mouse mammary glands and tumors. Total RNA was prepared from the indicated mammary tumors (T) or grossly normal mammary glands (N) of age-matched multiparous line 14 and 16 MMTV-c-*rel* mice. RNA samples (5 μg) were subjected to RPA analysis to assess mRNA levels for *cyclin A1, A2, B1, B2, C, D1, D2, and D3*, and L_{32} and *GAPDH* housekeeping genes. Data from two sets of analyses are shown in the left and right panels. The identities of the RNase protected bands were established using the undigested probes as markers and a control RNA for mouse *cyclin* mRNA expression provided with the kit (data not shown).

FIG. 8. MMTV-c-*rel* tumors overexpress c-*myc* RNA. A) Mammary glands. Total RNA was prepared from mammary glands of MMTV-*c-rel* transgenic mice and samples (15 μg) subjected to Northern analysis for c-*myc* mRNA expression. As a control, the gel was stained with ethidium bromide, shown below. The relative values of c-*myc* signal intensity normalized to levels of 28S rRNA are given relative to the WT (2) virgin sample. B) Mammary tumors. Total RNA was extracted from the indicated mammary tumors (T) and grossly normal mammary glands (N) of age-matched multiparous line 14 and 16 MMTV-c-*rel* mice. In addition, RNA was isolated from mammary glands of a nulliparous transgenic line 16 mouse (16 Virgin). RNA samples (20 μg) were subjected to Northern analysis for c-*myc* mRNA expression. As controls for RNA integrity and equal loading, the gel was stained with ethidium bromide, and RNA samples subjected to RT-PCR analysis for β-*actin* mRNA levels (see Fig. 6 above). The values of c-*myc* signal intensity normalized to 28S rRNA levels relative to the line 16 virgin sample are given below.

FIG. 9. EGCG inhibits growth of NF639 cells. NF639 cells were plated, in triplicate, at a density of 3.9×10^3 cells/cm^2. After overnight incubation, EGCG was added at the indicated concentration (μg/ml) dissolved in DMSO or with the volume of DMSO vehicle alone equivalent to the highest dose employed, as control (0 μg/ml). Cultures were incubated for an additional 24, 48 or 72 h. Cell proliferation was quantified using the Non-radioactive Proliferation Assay as measured by conversion of MTS dye to its formazan product read at OD490 nm. The data are presented as the mean +/- SD.

FIG. 10. EGCG inhibits growth of NF639 cells in soft agar. NF639 cells were plated, in triplicate, in soft agar at a density of 7.5×10^3 cells/ml in the absence or presence of the indicated concentration of EGCG. After 2 weeks, colonies were stained and three random fields counted from each of the triplicate samples. Average percent of control colony numbers per field +/- S.D. presented as a function of EGCG concentration. (Inset) Stained colonies were photographed using a Kodak digital camera.

FIG. 11. EGCG treatment of NF639 cells reduces NF-κB binding, and activities of PI 3-kinase and Akt kinases. NF639 cells were treated with either 40 μg/ml EGCG dissolved in DMSO for 24 h or with the equivalent amount of carrier solution. Alternatively, cells were incubated with 100 nM Wortmannin, a potent inhibitor of PI 3-kinase. A) NF-κB binding.

Nuclear extracts were prepared from EGCG-treated and control cells and used in EMSA with an oligonucleotide containing the URE NF-κB element upstream of the c-*myc* promoter, as probe (top panel) or with an Sp1 oligonucleotide, as a control for equal loading (bottom panel). The two major complexes seen were identified previously as p50 homodimers and p65/p50 heterodimers, as indicated. B) Akt kinase assay. WCEs were isolated with lysis buffer. For the kinase assay, samples containing 100 μg protein were immunoprecipitated overnight with a phospho-Akt antibody immobilized on beads, and bound proteins were used in a kinase assay with 1 μg GSK3α-GST protein as substrate. Phosphorylated GSK3α was identified by immunoblotting. C) PI 3-kinase assay. Samples of WCEs (50 μg) were subjected to immunoblotting for phosphorylated Akt, as a measure of PI-3 kinase activity. The blot was also probed for levels of β-actin, which indicated equal sample loading.

FIG. 12. EGCG reduces basal Her-2/neu phosphorylation in NF639, SMF and Ba/F3 2+4 cells. A) NF639 cells. NF639 cells were treated for 48 h with either 20, 40 or 80 μg/ml EGCG dissolved in DMSO or the equivalent amount of carrier DMSO. WCEs were isolated with lysis buffer. In the absence of good immunoprecipitating antibodies for mouse Her-2/neu, samples (50 μg) were subjected to immunoblot for Her-2/neu phosphorylation using an antibody that recognizes tyrosine-phosphorylated Her-2/neu specifically. The blot was also probed for levels of β-actin, which indicates equal sample loading. B) SMF and Ba/F3 cells. SMF and Ba/F3-2+4 cells were treated for 24 h with 40 μg/ml EGCG or the equivalent volume of carrier DMSO. WCEs were isolated with lysis buffer, and samples (50 μg) were subjected to immunoblotting for tyrosine phosphorylation, as above. The blot was also probed for levels of β-actin, which confirmed equal loading of the paired samples.

Appendix

1.   List of key research accomplishments (over the course of the grant):
-       NF-κB is functionally activated in HMECs malignantly transformed by environmental carcinogens
-       In premalignant HMECs immortalized by carcinogen treatment *in vitro,* NF-κB activity was dysregulated in quiescence.
-       Transgenic mice with targeted ectopic expression of the c-Rel subunit in the mammary gland were established (MMTV-c-*rel*), and a causal role of NF-κB in mammary tumorigenesis demonstrated.
-       MMTV-c-Rel cell lines have been established.
-       Aromatic Hydrocarbon Receptor (AhR) and RelA (p65) cooperate to transactivate the c-*myc* promoter in the untransformed and transformed breast epithelial cells.
-       Green tea polyphenol epigallocatechin-3 gallate (EGCG) was shown to inhibit Her-2/neu signaling, proliferation and transformed phenotype of breast cancer cells.

2.   Degrees Obtained
-       Ph.D. defense passed by the previous Principal Investigator (Dong Wook Kim). Formal degree to be awarded on June of 2001 upon completion of M.D. degree at Boston University School of Medicine.

3.   Manuscripts/Presentations (by original PI Dong Kim and current PI Shangqin Guo)
-       **D.W. Kim**, M.A. Sovak, G. J. Zanieski, G. Nonet, R. Romieu-Mourez, A. W. Lau, L.J. Haefer, P. Yaswen, M. Stampfer, A.E. Rogers, J. Russo,G.E. Sonenshein. Activation of NF-κB/Rel Occurs Early During Neoplastic Transformation of Mammary Cell. Carcinogenesis 21: 871-879 (2000).
-       **D. W. Kim,** L. Gazourian, S. A. Quadri, R. Romieu, D. H. Sherr, and G. E. Sonenshein. The Aromatic Hydrocarbon Receptor/Transcription Factor (AhR) and the p65 Nuclear Factor-κB Subunit Cooperate to Transactivate the c-*myc* Promoter. Oncogene 19: 5498-5506 (2000).
-       **D. W. Kim,** M.A. Sovak, G. Zanieski, A. Lau, L.Gazourian, S. A. Quadri, R. Romieu-Mourez, G. Nonet, L.J. Haefer, P. Yaswen, M. Stampfer, J. Russo, A. E. Rogers, P. Toselli, D. Sherr, and G. E. Sonenshein. Role of NF-κB/Rel, AhR and c-Myc in breast cancer. DOD ERA of Hope Conference 2001, Atlanta GA.
-       **D.W. Kim**, M.A. Sovak, M. Arsura, G. J. Zanieski, K. Kavanagh, G. Nonet, P. Yaswen, M. Stampfer, J. Russo, A.E. Rogers, G.E. Sonenshein. Early Activation of NF-κB/Rel During Neoplastic Transformation of Mammary Cells. Russek Day Presentation, Boston University School of Medicine (2nd Prize Award).
-       **S. Guo**, S. Pianetti, K.T. Kavanagh, and G.E. Sonenshein. Green tea polyphenol epigallocatechin-3 gallate inhibits Her-2/neu signaling, proliferation and transformed phenotype of breast cancer cells. 41st ASCB Meeting, 2001. Washington DC.
-       S. Pianetti*, **S. Guo***, K.T. Kavanagh, and G.E. Sonenshein. Green tea polyphenol epigallocatechin-3 gallate inhibits Her-2/neu signaling, proliferation and transformed phenotype of breast cancer cells. Cancer Research 62, 652-655 (2002). *The authors contributed equally.

Table 1. Tumor incidence and histopathology in female MMTV-c-*rel* transgenic mice after multiple cycles of pregnancy and regression[a].

Mammary Tumor Diagnosis (Other Tumors)[b]	Age[c] (mo.)	# Mam. Tum.[d]	Other Tum.	Line[a]	Mouse[e] #
Mam. squamous cell carcinoma & hyperplasia (bronch. adenocarcinoma)	22	1	1	7	4026
Mam. adenosquamous carcinoma	22	1	0	7	4042
Mam. adenosquamous carcinoma	18	1	0	14	3814
Mam. adenosquamous carcinoma (papillary bronch. adenomas)	20	1	1	14	3983
Mam. adenocarcinomas with pulmonary metastases	23	4	1	14	3996
Mam. papillary carcinoma, lobular hyperplasia, squamous nodules	23	1	0	14	4936
Mam. squamous cell carcinoma & hyperplasia	15	1	0	14	4556
Mam. adenocarcinoma (papillary bronchial adenocarcinomas)	19	1	1	15	127
Mam. squamous cell carcinoma	22	1	0	16	3872
Mam. adenocarcinoma with poorly differentiated large cell	18	1	0	16	3875
Mam. squamous cell carcinoma & hyperplasia (centrocytic lymphoma)	18	1	1	16	4521
Spindle cell tumor, originating from a mammary adenocarcinoma	19	1	0	16	4528

[a]Thirty-eight multiparous female mice from the 4 transgenic lines (7, 14, 15 and 16) were monitored for tumor incidence by bi-weekly palpable examination. [b]Histopathological analysis of mammary glands and other organs (heart, lung, liver, kidney, spleen and adrenal gland) from the same animal was performed when presence of a tumor was detected. [c]Age of transgenic mouse (in months) at the time the mammary tumor was detected. [d]Number of mammary tumors observed. [e]An identification number was given to the individual mice of the cohort for further analysis of the tumors, as shown below.
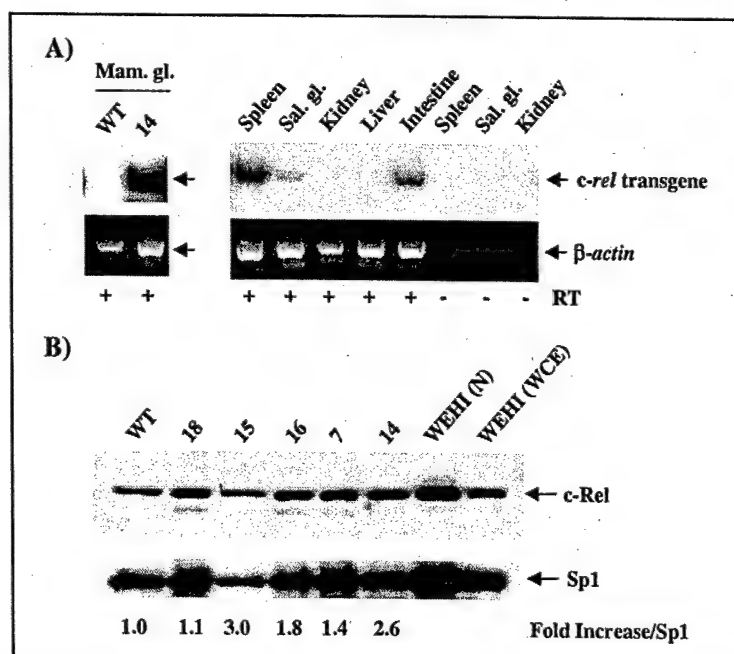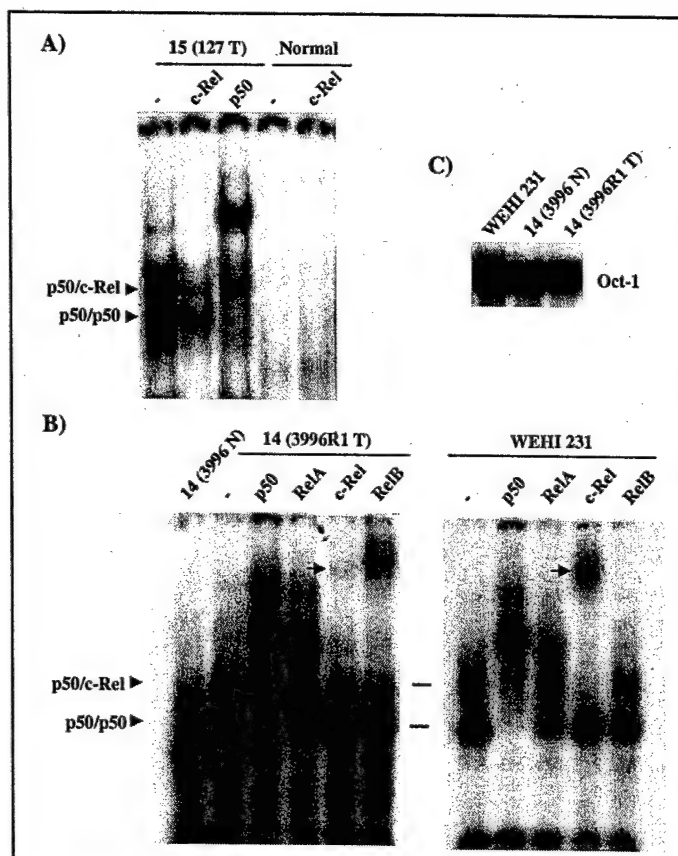

Figure 1.

Figure 2

Figure 3

A)

c-*rel* transgene

β-*actin*

B)

Tumors

c-Rel

Coomassie

Figure 4

A)

15 (127 T)   Normal

p50/c-Rel
p50/p50

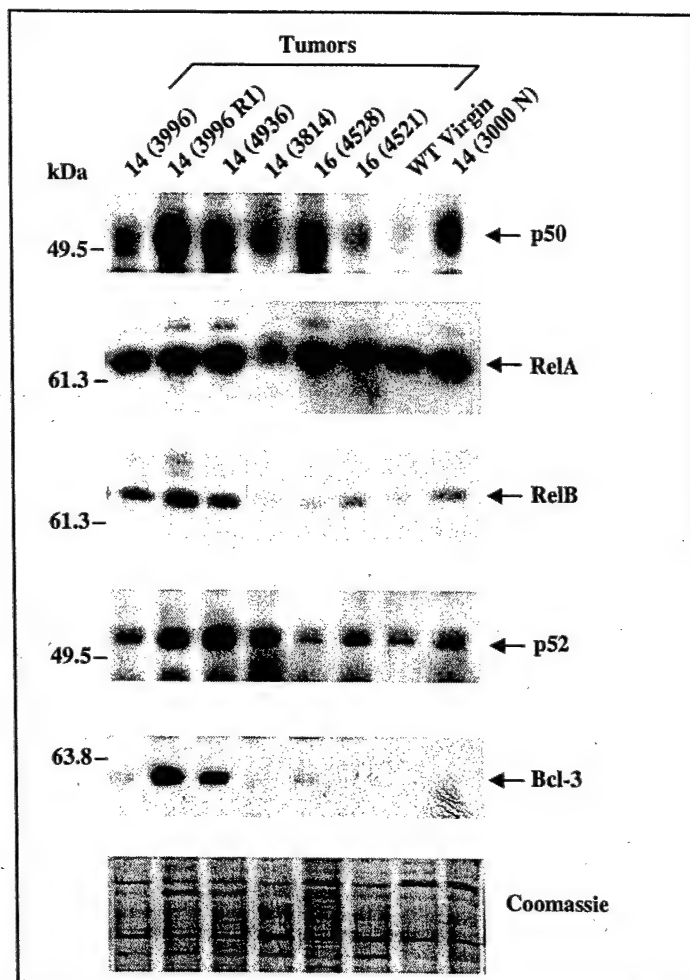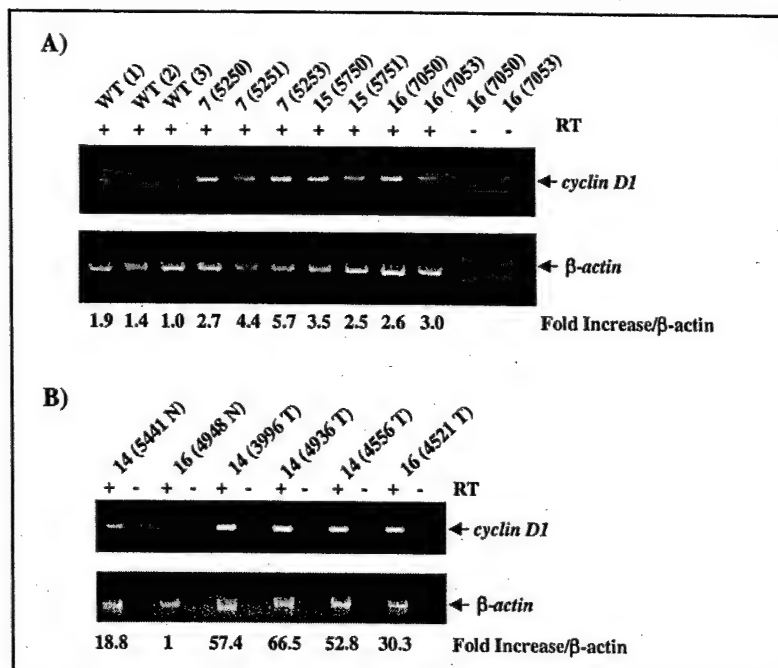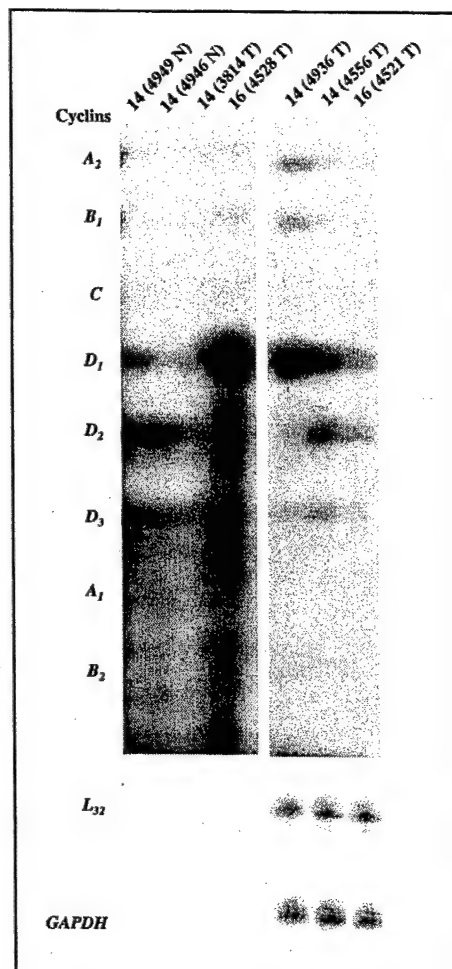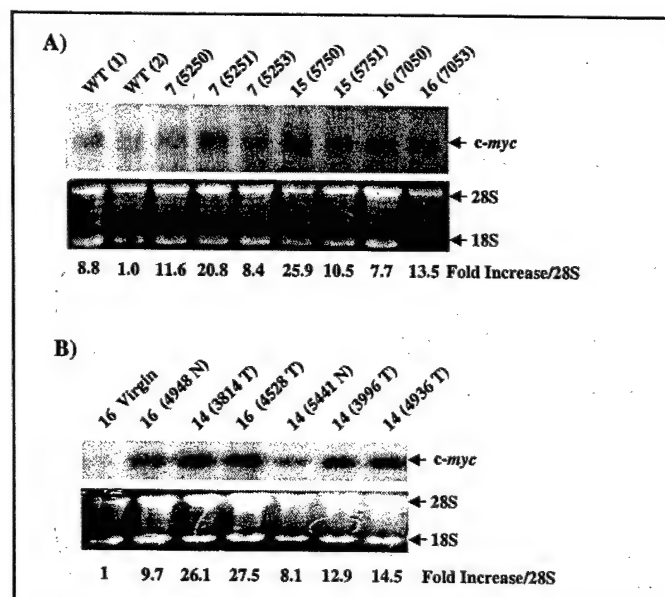C)

Oct-1

B)

14 (3996R1 T)   WEHI 231

p50/c-Rel
p50/p50
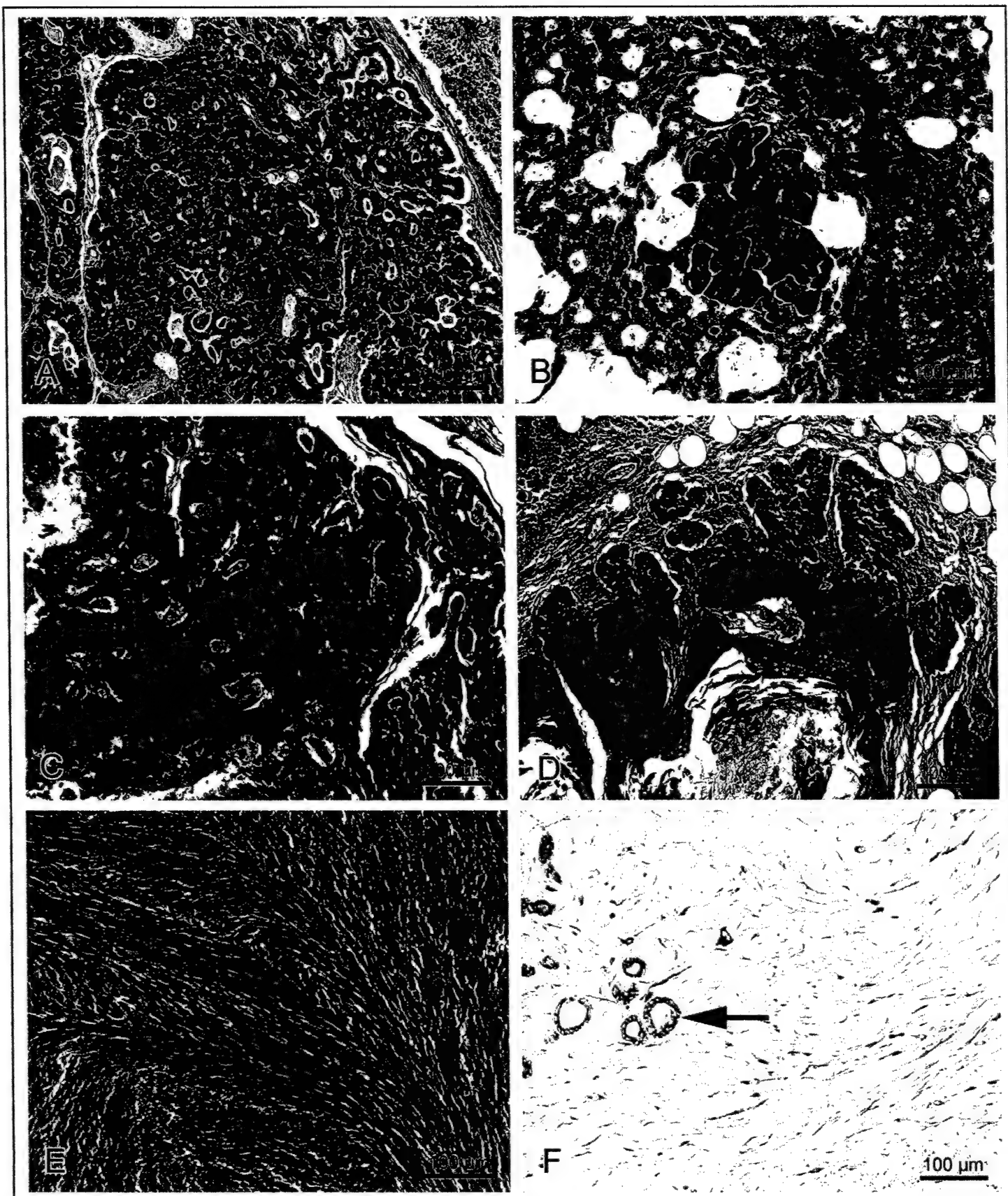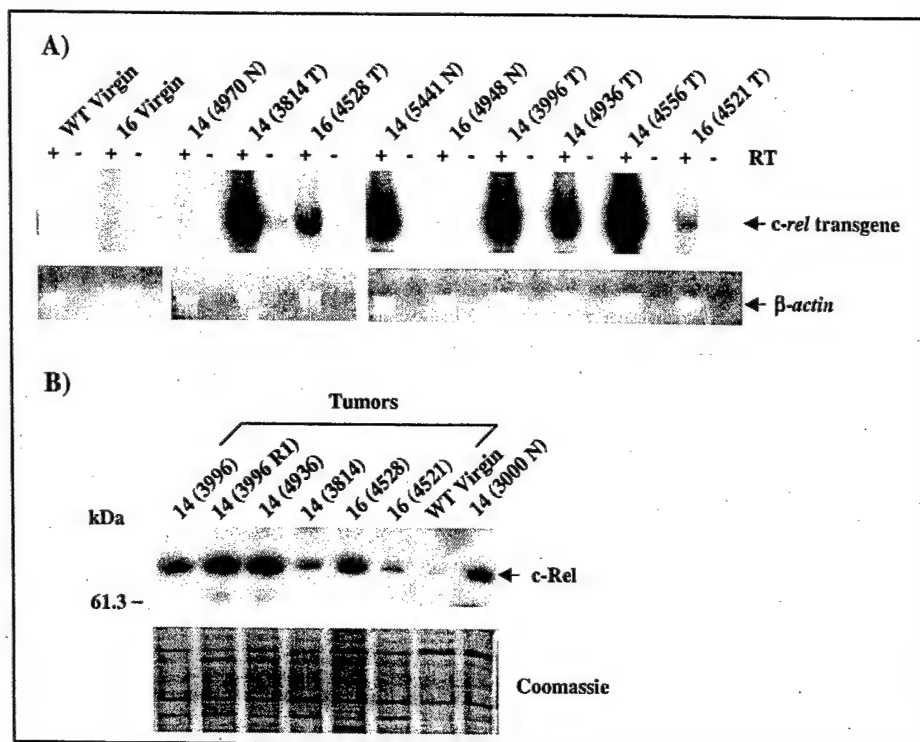
Figure 5

Figure 6

Figure 7

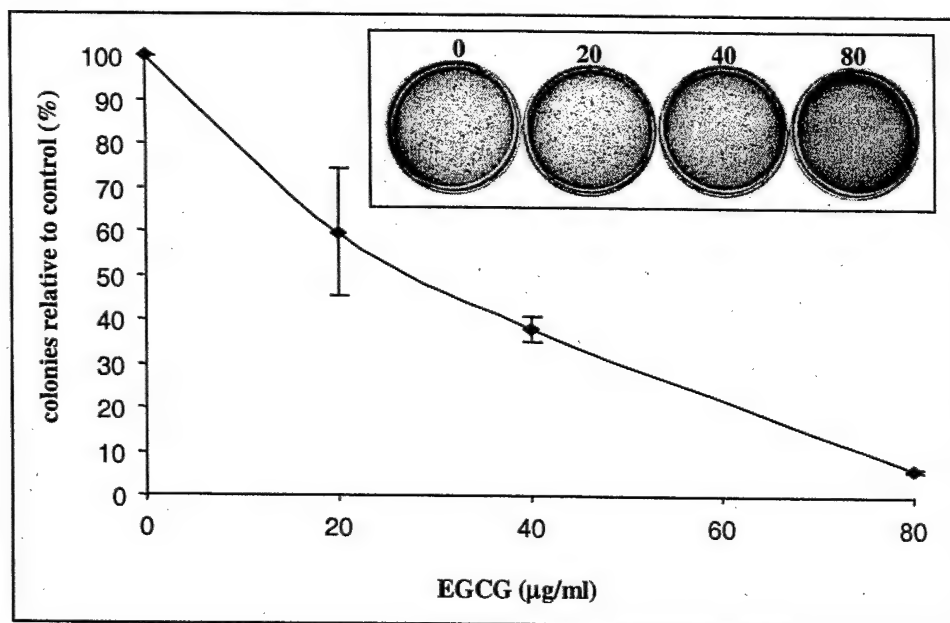
Figure 8
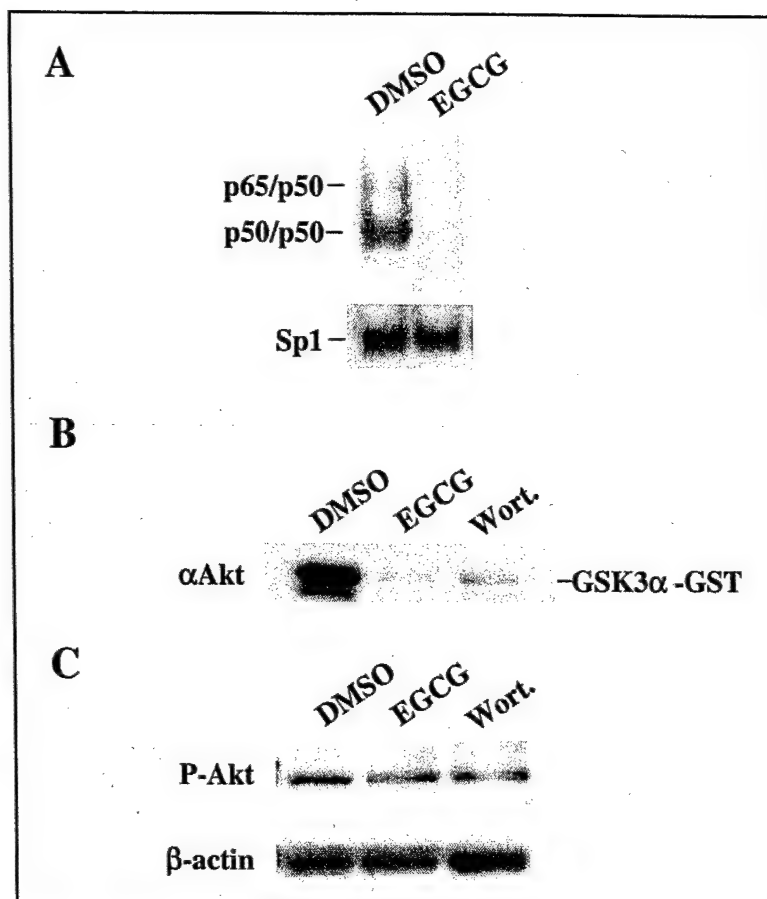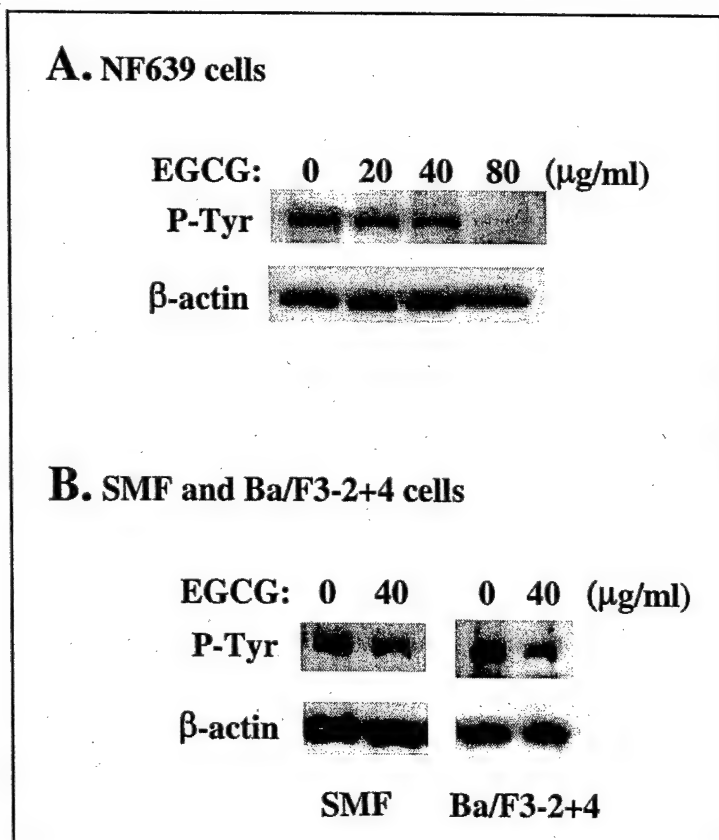
Figure 9
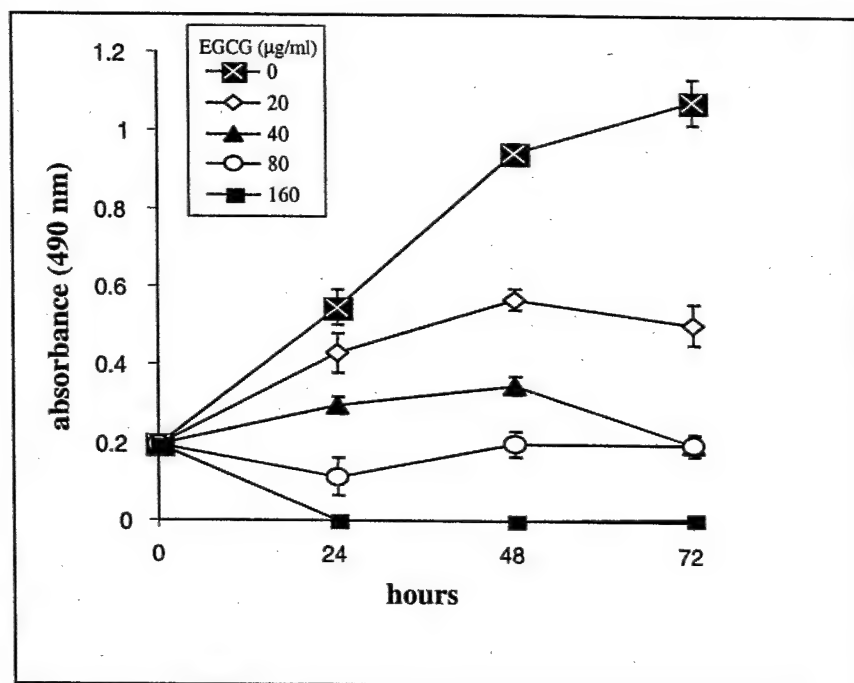
Figure 10

Figure 11

Figure 12

Advances in Brief

Green Tea Polyphenol Epigallocatechin-3 Gallate Inhibits Her-2/Neu Signaling, Proliferation, and Transformed Phenotype of Breast Cancer Cells[1]

Stefania Pianetti,[2] Shangqin Guo,[2] Kathryn T. Kavanagh, and Gail E. Sonenshein[3]

Departments of Biochemistry [S. P., S. G., G. E. S.], and Pathology and Laboratory Medicine [K. T. K.], and Program in Research on Women's Health [S. P., S. G., K. T. K., G. E. S.], Boston University School of Medicine, Boston, Massachusetts 02118-2394

Abstract

Overexpression of the epidermal growth factor receptor family member Her-2/neu in breast cancer is associated with poor prognosis. With evidence accumulating for a chemopreventive role of green tea polyphenols, the effects of epigallocatechin-3 gallate (EGCG) on Her-2/neu-overexpressing breast cancer cells were examined. EGCG inhibited mouse mammary tumor virus (MMTV)-Her-2/neu NF639 cell growth in culture and soft agar. EGCG reduced signaling via the phosphatidylinositol 3-kinase, Akt kinase to NF-κB pathway because of inhibition of basal Her-2/neu receptor tyrosine phosphorylation. EGCG similarly inhibited basal receptor phosphorylation in SMF and Ba/F3 2 + 4 cells, which suggests the potential beneficial use of EGCG in adjuvant therapy of tumors with Her-2/neu overexpression.

Introduction

The *Her-2/neu* (or *c-erbB-2*) oncogene, which is the second member of the EGFR[4] family (EGFR-2), encodes a transmembrane tyrosine receptor kinase. Overexpression of Her-2/neu, which has been seen in ~30% of breast cancers, is associated with poor overall survival (1). In particular, it has been found associated with increased metastatic potential and resistance to chemotherapeutic agents. Transgenic mice overexpressing Her-2/neu develop focal mammary tumors (2). Recent work has implicated the PI 3-kinase to serine/threonine kinase Akt/protein kinase B to NF-κB signaling pathway in control of growth and transformed phenotype of Her-2/neu-overexpressing cells (3–5). Green tea is rich in polyphenols, such as EGCG, that possess antioxidant qualities, which have been shown to have anticarcinogenic activity against a variety of tumor types including breast cancer (reviewed in Ref. 6). For example, we recently showed that female rats given green tea as their drinking fluid displayed a significant decrease in carcinogen-induced mammary tumor burden and invasiveness and significantly increased latency to first tumor (7). Doses of either green tea polyphenol mix or EGCG between ~40 to 80 μg/ml slowed growth of various estrogen receptor-negative breast cancer cell lines in culture (7). Furthermore, statistics indicate that the incidence of breast cancer in regions in which green tea is consumed in large quantities, including China and Japan, is much lower than in western societies. Here we have examined the effects of EGCG on Her-2/neu-overexpressing breast cancer cells. We report that treatment of MMTV-Her-2/neu mouse mammary tumor NF639 cells with EGCG slows proliferation and reduces growth in soft agar via inhibiting the PI 3- to Akt kinase to NF-κB pathway. EGCG-reduced basal receptor tyrosine phosphorylation in NF639 and two other Her-2/neu-overexpressing lines. These findings suggest the use of EGCG may be beneficial in chemoprevention of breast cancer and represents a possible tool in adjuvant therapy modalities of patients with tumors overexpressing the Her-2/neu receptor.

Materials and Methods

Cell Growth and Treatment Conditions. The MMTV-Her-2/neu cell lines NF639 and SMF (kindly provided by P. Leder, Harvard Medical School, Boston, MA) were derived from mammary gland tumors and cultured as described previously (8). Ba/F3 pro-B cells, which are transfected to express Her-2/neu and EGFR-4 (Ba/F3–2 + 4), were kindly provided by David Stern (Yale University, New Haven, CN; Ref. 9). These cells, which display high constitutive Her-2/neu phosphorylation (5), were grown in RPMI supplemented with 10% fetal bovine serum, conditioned medium from WEHI 3 cells, and antibiotics, as described previously (9). EGCG, purchased from LKT Laboratories Inc. (St Paul, MN), was dissolved in sterile 50% DMSO at a concentration of 100 mg/ml, and diluted with double-distilled H_2O to a 1 mg/ml working-strength solution. Nonradioactive MTS cell proliferation assays (Promega) were performed essentially as we have published previously (7).

EMSA. Nuclear extracts were prepared from breast cancer cells in extraction buffer [420 mM KCl, 20 mM HEPES (pH 7.9), 1.5 mM $MgCl_2$, 0.2 mM EDTA, and 20% glycerol] plus protease inhibitors (0.5 mM DTT, 0.5 mM PMSF, and 10 μg/ml LP), as we have published previously (5). The sequence of the URE NF-κB-containing oligonucleotide from the c-*myc* gene is as follows: 5′-GATCCAAGTCCGGGTTTTCCCCAACC-3′, in which the underlined region indicates the core binding element. The sequence of the Sp1 oligonucleotide is 5′-ATTCGATCGGGGCGGGGCGACC-3′. Oligonucleotides were end labeled with large Klenow fragment of DNA polymerase and [^{32}P]dNTPs. The EMSA was performed using 5 μg of nuclear extract, essentially as we have published previously (5).

Akt Kinase Assay. The Akt kinase assay, was performed following the directions of the Akt Kinase Assay kit (New England Biolabs, Beverly, MA). Briefly, samples (100-μg) of WCEs were immunoprecipitated overnight with an agarose conjugated anti-Akt antibody (New England Biolabs) at 4°C. The immunoprecipitate was resuspended in kinase buffer, and the assay performed at 30°C for 45 min, using 1 μg of GSK3α-GST fusion protein as substrate in the presence of 10 μM ATP. The resulting products were resolved in a 10% polyacrylamide-SDS gel and subjected to immunoblotting, as below, using phosphospecific GSK-3α antibody (New England Biolabs).

Immunoblot Analysis. Cells were rinsed with cold PBS, and harvested in lysis buffer [50 mM Tris-HCl (pH 8.0), 5 mM EDTA (pH 8.0), 150 mM NaCl, 0.5 mM DTT, 2 μg/ml aprotinin, 2 μg/ml LP, 0.5 mM PMSF, 0.5% and NP40]. WCEs were obtained by sonication, followed by centrifugation at 14,000 rpm for 30 min. Samples were subjected to electrophoresis in a 10% polyacrylamide-SDS gel and immunoblotting, as previously described (5). Antibodies used were: phosphorylated Akt Ser473 (Cell Signaling) and tyrosine phospho-

rylated Her-2/neu (Santa Cruz Biotechnology), and β-actin (Sigma Chemical Co.).

Focus Formation Assay. NF639 cells were plated, in triplicate, at 7.5×10^3/ml in top plugs consisting of complete medium and 0.4% SeaPlaque agarose (FMC Bioproducts, Rockland, ME) with the indicated concentration of EGCG. Plates were subsequently incubated for 2 weeks in humidified incubator at 37°C. Cells were stained with 2 ml of crystal violet solution and washed extensively with water, and colonies were counted using an inverted bright field microscope at a ×2 magnification. Three random fields were counted from each of the triplicate samples, and average values presented ± SD, which was determined in each set of nine values obtained using the Student's t test.

Transfection Analysis. Twenty-four h after plating at 30% confluence in P150 dishes, NF639 cells were transfected with 5 μg of NF-κB-element-driven luciferase reporter DNA (10), kindly provided by Georges Rawadi (Hoescht-Marion-Roussel, Romainville, France) with 25 μg of pcDNA empty vector in 45 μl of FuGENE Reagent. Three h after transfection, cells were trypsinized and replated in multiple P60 dishes. After overnight incubation, cells were treated in duplicate with either 50 μg/ml EGCG or carrier DMSO solution for 24 h. Cells were harvested and extracts assayed for luciferase activity as described previously (5). Averages values are presented ± SD. SD was obtained using the Student's t test.

Results

EGCG Inhibits Growth of MMTV-Her-2/neu Breast Cancer Cell Lines. We first tested the ability of EGCG to inhibit growth of the MMTV-Her-2/neu mouse breast tumor derived cell line NF639. Cultures were plated, in triplicate, at a density of 3.9×10^3 cells/cm^2. After 24 h, EGCG was added to a final concentration of 20–160 μg/ml, or the volume of carrier DMSO equivalent to the highest dose was added. Cell growth was assessed every 24 h using a nonradioactive MTS cell proliferation assay (Fig. 1). A dose-dependent decrease in the rate of proliferation was seen with 20 and 40 μg/ml EGCG, whereas no cell growth was seen with 80 μg/ml EGCG. On treatment with 160 μg/ml EGCG, a drop in cell numbers was seen. This suggested that extensive death of NF639 cells was occurring only at this higher dose, which was confirmed by trypan blue staining of cells with 0, 40, 80, or 160 μg/ml EGCG (data not shown). Thus, treatment of the NF639 breast tumor cells with 20–80 μg/ml EGCG decreases their rate of proliferation in culture.

EGCG Inhibits Growth of NF639 Cells in Soft Agar. Growth in soft agar is a hallmark of transformed phenotype. Hence, we next
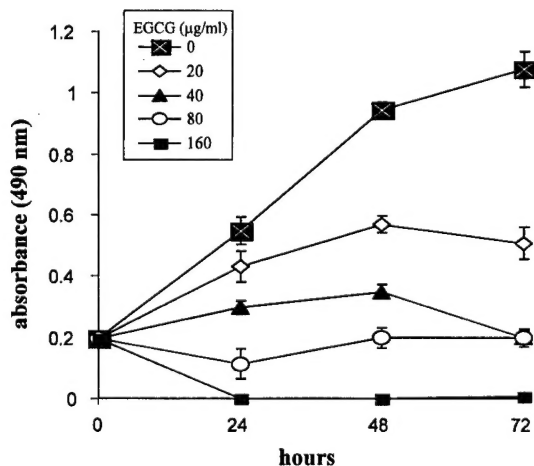
Fig. 1. EGCG inhibits growth of NF639 cells. NF639 cells were plated, in triplicate, at a density of 3.9×10^3 cells/cm^2. After overnight incubation, EGCG was added at the indicated concentration (μg/ml) dissolved in DMSO or with the volume of DMSO vehicle alone equivalent to the highest dose used, as control (0 μg/ml). Cultures were incubated for an additional 24, 48, or 72 h. Cell proliferation was quantified using the nonradioactive proliferation assay as measured by conversion of MTS dye to its formazan product read at $A_{490\,nm}$. The data are presented as the mean ± SD.
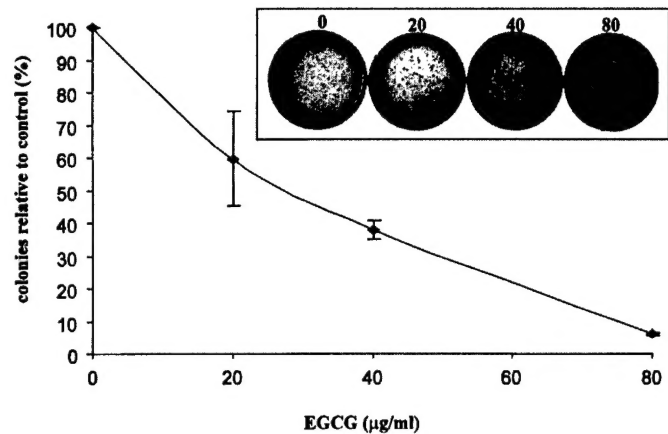
Fig. 2. EGCG inhibits growth of NF639 cells in soft agar. NF639 cells were plated, in triplicate, in soft agar at a density of 7.5×10^3 cells/ml in the absence or presence of the indicated concentration of EGCG. After 2 weeks, colonies were stained and three random fields counted from each of the triplicate samples. Average percentage of control colony numbers per field ± SD presented as a function of EGCG concentration. *Inset*, stained colonies were photographed using a Kodak digital camera.

assessed the ability of EGCG to reduce growth of NF639 cells in soft agar. NF639 cells were plated, in triplicate, at a density of 7.5×10^3 cells/ml in top plugs consisting of complete medium and 0.4% Sea-Plaque agarose containing 0, 20, 40 or 80 μg/ml EGCG. The plates were incubated for two weeks and colonies stained with crystal violet and counted as described in the "Materials and Methods." A decrease in colony numbers was seen which was more pronounced with increasing doses of EGCG (Fig. 2, inset). Quantitation of the results confirmed that the inhibition of colony formation occurred in a dose-dependent fashion with EGCG treatment (Fig. 2). Thus, EGCG inhibits growth in soft agar, an important property of the transformed phenotype.

EGCG Reduces NF-κB Activity in the NF639 Cell Line. To assess the effects of EGCG on Her-2/neu signaling, we first monitored the recently identified downstream target NF-κB (5). NF639 cells were treated with 40 μg/ml EGCG for 24 h and nuclear extracts prepared. These were used in EMSA with an oligonucleotide containing the NF-κB element upstream of the c-*myc* promoter. Extracts from DMSO-treated cells gave rise to two bands (Fig. 3A). These have been identified previously as containing complexes composed of p65/p50 and p50 homodimers (p50/p50; 5). Incubation in the presence of 40 μg/ml EGCG reduced formation of both of these two complexes. This decrease was selective, because no change was seen in Sp-1 binding (Fig. 3A). We next assessed the effects of EGCG on NF-κB activity. A transfection assay was performed using an NF-κB element-driven luciferase reporter. In two experiments, treatment with 50 μg/ml EGCG for 24 h reduced NF-κB activity by 76.3% ± 5.9%. Thus, EGCG inhibits NF-κB binding and activity in NF639 cells.

EGCG Inhibits the PI 3- to Akt Kinase Signaling Pathway. Previously, we showed that induction of NF-κB in NF639 cells occurs via a PI 3-kinase-to-Akt-kinase pathway (5). To test the effect of EGCG treatment on Akt phosphorylation, the cells were incubated for 24 h in the presence of either 40 μg/ml of EGCG that had been dissolved in DMSO or the equivalent amount of carrier solution. Alternatively, cells were incubated in the presence of 100 nM Wortmannin, a potent specific inhibitor of PI 3-kinase (11). WCEs were prepared and immunoprecipitated with a monoclonal anti-Akt, which preferentially recognizes phosphorylated protein. GSK3α-GST was then used as the substrate for the resulting immunoprecipitated Akt, and the phosphorylated material identified by immunoblot analysis for phosphorylated GSK3α-GST protein (Fig. 3B). The EGCG treatment
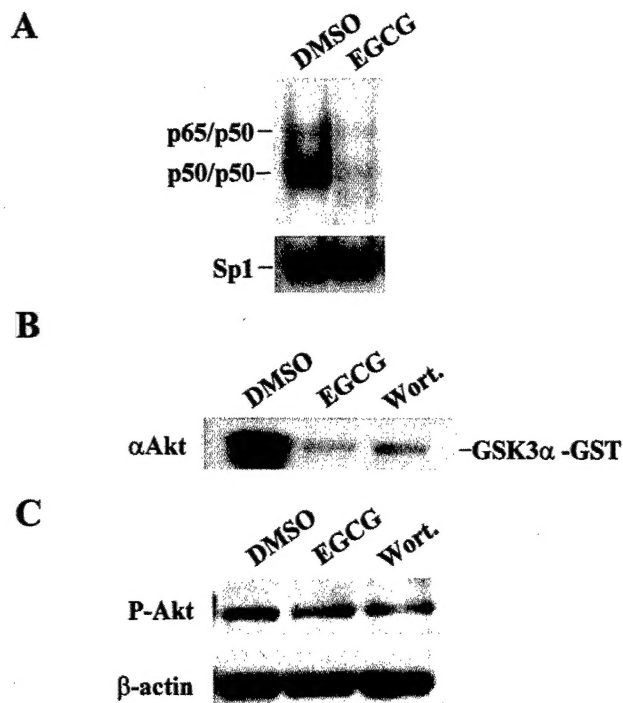
A

p65/p50—
p50/p50—

Sp1—

B

αAkt   —GSK3α -GST

C

P-Akt

β-actin

Fig. 3. EGCG treatment of NF639 cells reduces NF-κB binding and activities of PI 3- and Akt kinases. NF639 cells were treated with either 40 μg/ml EGCG dissolved in DMSO for 24 h or with the equivalent amount of carrier solution. Alternatively, cells were incubated with 100 nM Wortmannin, a potent inhibitor of PI 3-kinase. A, NF-κB binding. Nuclear extracts were prepared from EGCG-treated and control cells and used in EMSA with an oligonucleotide containing the URE NF-κB element upstream of the c-myc promoter, as probe (top panel) or with an Sp1 oligonucleotide, as a control for equal loading (bottom panel). The two major complexes seen were identified previously as p50 homodimers and p65/p50 heterodimers, as indicated previously (5). B, Akt kinase assay. WCEs were isolated with lysis buffer. For the kinase assay, samples containing 100 μg protein were immunoprecipitated overnight with a phospho-Akt antibody immobilized on beads, and bound proteins were used in a kinase assay with 1 μg GSK3α-GST protein as substrate. Phosphorylated GSK3α was identified by immunoblotting. C, PI 3-kinase assay. Samples of WCEs (50 μg) were subjected to immunoblotting for phosphorylated Akt, as a measure of PI-3 kinase activity. The blot was also probed for levels of β-actin, which indicated equal sample loading.

resulted in a dramatic decrease in phosphorylated GSK3α-GST. A similar decrease was observed with Wortmannin treatment.

As a test for the effects of EGCG on PI 3-kinase activity, we measured the presence of phosphorylated Akt, which is one of its critical signaling substrates. Immunoblotting was performed using an antibody specific for phospho-Akt (Ser473). Treatment with EGCG caused an ~50% decrease in phosphorylated Akt protein (Fig. 3C). A similar level of decrease was observed on treatment with Wortmannin, which suggested that the remaining phosphoprotein detected is attributable to other kinase activities. Immunoblotting for β-actin confirmed equal loading. Together, these results demonstrate the ability of EGCG to reduce the activities of both PI 3-kinase and Akt.

EGCG Reduces Basal Phosphorylation of Her-2/neu. Overexpression of Her-2/neu can lead to constitutive phosphorylation and basal receptor activation and signaling. Thus, we tested whether treatment with EGCG can reduce this basal Her-2/neu phosphorylation. NF639 cells were treated with 0, 20, 40, or 80 μg/ml EGCG for 48 h. WCEs were isolated and subjected to immunoblot analysis using a tyrosine phosphospecific Her-2/neu antibody (Fig. 4A). A dose-dependent drop in phosphorylated Her-2/neu protein was noted. Densitometry indicated treatment with 20, 40, or 80 μg/ml caused a decrease of 13, 38, and 96%, respectively compared with control cells. Immunoblotting for β-actin confirmed equal loading. To verify that this effect was general, we analyzed two additional cell lines: (a) SMF
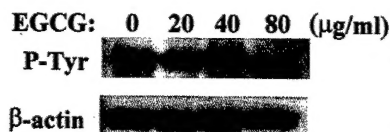
cells, similarly derived from an MMTV-Her-2/neu mouse mammary tumor (8); and (b) Ba/F3 2 + 4 cells, a pro-B cell line clone stably expressing Her-2/neu + EGFR-4 (5, 9), displaying high constitutive Her-2/neu activity (5). SMF and Ba/F3 2 + 4 cells were treated with 40 μg/ml EGCG for 24 h and analyzed by immunoblotting for phosphorylated Her-2/neu (Fig. 4B). EGCG treatment similarly reduced basal phosphorylation of Her-2/neu in both cell lines. Thus, EGCG reduces the basal phosphorylation and constitutive activation of the Her-2/neu receptor.

Discussion

Here we show that the green tea polyphenol EGCG inhibits the signaling by Her-2/neu that promotes cell proliferation, survival, and transformed phenotype. Treatment of MMTV-Her-2/neu mammary gland tumor NF639 cells with doses of EGCG up to 80 μg/ml slowed growth and dramatically reduced colony formation in soft agar with little effect on cell viability. Higher doses (160 μg/ml) reduced cell numbers and induced cell death as judged by trypan blue assays. Previously, we demonstrated that the overexpression of Her-2/neu in NF639 cells leads to the induction of NF-κB via a PI 3-kinase/Akt kinase signaling pathway (5). EGCG inhibited this Her-2/neu signaling as judged by the observed decreases in PI 3-kinase, Akt kinase, and NF-κB activities. Furthermore, EGCG inhibited constitutive Her-2/neu phosphorylation in NF639 cells, as well as in SMF cells, a second mouse MMTV-Her-2/neu tumor-derived cell line, and Ba/F3 2 + 4 cells, a pro-B cell line transfected to express Her-2/neu + EGFR-4. Overall, these studies demonstrate for the first time that EGCG can ablate the Her-2/neu signaling cascade in breast cancer cells, by reducing basal Her-2/neu receptor phosphorylation. These results suggest further study of the potential role of EGCG in adjuvant therapy treatment modalities and of green tea components in chemoprevention of breast cancer are warranted.

In animal models, green tea extracts have been shown to inhibit chemical and photo carcinogenesis. For example, green tea was found to inhibit cancers of the gastrointestinal tract, lung, and skin in mice

A. NF639 cells

EGCG: 0 20 40 80 (μg/ml)

P-Tyr

β-actin

B. SMF and Ba/F3-2+4 cells

EGCG: 0 40   0 40 (μg/ml)

P-Tyr
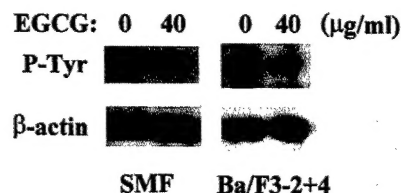
β-actin

SMF   Ba/F3-2+4

Fig. 4. EGCG reduces basal Her-2/neu phosphorylation in NF639, SMF, and Ba/F3 2 + 4 cells. A, NF639 cells. NF639 cells were treated for 48 h with either 20, 40, or 80 μg/ml EGCG dissolved in DMSO or the equivalent amount of carrier DMSO. WCEs were isolated with lysis buffer. In the absence of good immunoprecipitating antibodies for mouse Her-2/neu, samples (50 μg) were subjected to immunoblot for Her-2/neu phosphorylation using an antibody that recognizes tyrosine-phosphorylated Her-2/neu specifically. The blot was also probed for levels of β-actin, which indicates equal sample loading. B, SMF and Ba/F3 cells. SMF and parental and Ba/F3-2 + 4 cells were treated for 24 h with 40 μg/ml EGCG or the equivalent volume of carrier DMSO. WCEs were isolated with lysis buffer, and samples (50 μg) were subjected to immunoblotting for tyrosine phosphorylation, as above. The blot was also probed for levels of β-actin, which confirmed equal loading of the paired samples.

(reviewed in Ref. 6). It has been reported also that EGCG inhibits the growth of human breast and prostate tumors transplanted into athymic mice (12). We recently demonstrated that green tea extracts given to female Sprague Dawley rats in their drinking fluid significantly decrease DMBA-induced mammary tumor burden and invasiveness and significantly increase latency to first tumor (7). Another study using a diet containing 1% green tea catechins fed to female Sprague Dawley rats showed that tea was effective in reducing mammary gland tumorigenesis in the promotion, but not the progression, stages of carcinogenesis (13). Consistent with these findings, several studies have also found that green tea treatment of breast cancer cells *in vitro* reduces their rate of proliferation (7, 14, and references therein). Overall, the toxicity of green tea extracts is low, and, thus, they represent potentially useful cancer chemopreventive agents.

Here, EGCG was shown to reduce NF-κB levels and activity in NF639 cells because of its ability to inhibit the Her-2/neu signaling pathway that leads to NF-κB activation. Further insight into the regulatory mechanisms will be provided when the endogenous downstream targets of NF-κB responding to EGCG treatment are elucidated. Our findings are consistent with previous observations on the ability of EGCG to block signaling by the EGFR family (15, 16). For example, Liang *et al.* (15) demonstrated the ability of EGCG to block EGF signaling via the EGFR in A431 epidermoid carcinoma cells. Interestingly, we observed cooperative inhibition of NF-κB binding levels on EGCG cotreatment with an antibody against the Her-2/neu receptor.[5] Yang *et al.* (17) observed that green tea polyphenols, including EGCG, could inhibit activated IκB kinase in the intestinal epithelial cell line IEC-6. Green tea extracts have also been found to block NF-κB activation in cancer cells on tumor necrosis factor-α, lipopolysaccharide, or UV treatment (18, 19). In contrast, EGCG failed to reduce NF-κB levels in Hs578T breast cancer cells[6] that were derived from a carcinosarcoma and display constitutive IκB kinase activation and elevated levels of protein kinase CK2 (formerly casein kinase II) that promote increased NF-κB activity (20). Thus, different signaling pathways display variable sensitivities to EGCG. Of note, the basal activation of Her-2/neu seems sensitive to EGCG inhibition.

Acknowledgments

References

1. Hortobagyi, G. N., Hung, M-C., and Buzdar, A. U. Recent developments in breast cancer therapy. Semin. Oncol., *26:* 11–20, 1999.

2. Guy, C. T., Webster, M. A., Schaller, M., Parson, T. J., Cardiff, R. D., and Muller, W. J. Expression of the *neu* proto-oncogene in the mammary epithelium of transgenic mice induces metastatic disease. Proc. Natl. Acad. Sci. USA, *89:* 10578–10582, 1992.

3. Ignatoski, K. M., Maehama, T., Markwart, S. M., Dixon, J. E., Livant, D. L., and Ethier, S. P. ERBB-2 overexpression confers PI 3′ kinase-dependent invasion capacity on human mammary epithelial cells. Br. J. Cancer, *82:* 666–674, 2000.

4. Ozes, O. N., Mayo, L. D., Gustin, J. A., Pfeffer, S. R., Pfeffer, L. M., and Donner, D. B. NF-κB activation by tumour necrosis factor requires the Akt serine-threonine kinase. Nature (Lond.), *401:* 82–85, 1999.

5. Pianetti, S., Arsura, M., Romieu-Mourez, R., Coffey, R. J., and Sonenshein, G. E. Her-2/neu overexpression induces NF-κB via a PI3-kinase/Akt pathway without IKK activation that can be inhibited by the tumor suppressor PTEN. Oncogene, *20:* 1287–1299, 2001.

6. Dreosti, I. E., Wargovich, M. J., and Yang, C. S. Inhibition of carcinogenesis by tea: the evidence from experimental studies. Crit. Rev. Food Sci. Nutr., *37:* 761–770, 1997.

7. Kavanagh, K. T., Hafer, L. G., Kim, D. W., Mann, K. K., Sherr, D. H., Rogers, A. E., and Sonenshein, G. E. Green tea extracts decrease carcinogen-induced mammary tumor burden in rats and rate of breast cancer cell proliferation in culture. J. Cell. Biochem., *82:* 387–398, 2001.

8. Elson, A., and Leder, P. Protein-tyrosine phosphatase ϵ. J. Biol. Chem., *279:* 26116–26122, 1995.

9. Riese, D. J., II, Kim, E. D., Elenius, K., Buckley, S., Klagsbrun, M., Plowman, G. D., and Stern, D. F. The epidermal growth factor receptor couples transforming growth factor-α, heparin-binding epidermal growth factor-like factor, and amphiregulin to Neu, ErbB-3, and ErbB-4. J. Biol. Chem., *271:* 20047–20052, 1996.

10. Rawadi, G., Zugaza, J. L., Lemercier, B., Marvaud, J. C., Popoff, M., Bertoglio, J., and Roman-Roman, S. Involvement of small GTPases in *Mycoplasma fermentans* membrane lipoproteins-mediated activation of macrophages. J. Biol. Chem., *274:* 30794–30798, 1999.

11. Arcaro, A., and Wymann, M. P. Wortmannin is a potent phosphatidylinositol 3-kinase inhibitor: the role of phosphatidylinositol 3,4,5-trisphosphate in neutrophil responses. Biochem. J., *296:* 297–301, 1993.

12. Liao, S., Umekita, Y., Guo, J., Kokontis, J. M., and Hiipakka, R. A. Growth inhibition and regression of human prostate and breast tumors in athymic mice by tea epigallocatechin gallate. Cancer Lett., *96:* 239–245, 1995.

13. Hirose, M., Hoshiya, T., Akegi, K., Futakuchi, M., and Ito, N. Inhibition of mammary gland carcinogenesis by green tea catechins and other naturally occurring antioxidants in female Sprague-Dawley rats pretreated with 7, 12-dimethylbenz(a)anthracene. Cancer Lett., *83:* 149–156, 1994.

14. Araki, R., Inoue, S., Osborne, M. P., and Telang, N. T. Chemoprevention of mammary preneoplasia. *In vitro* effects of a green tea polyphenol. Ann. N.Y. Acad. Sci., *768:* 215–222, 1995.

15. Liang, Y. C., Lin-shiau, S. Y., Chen, C. F., and Lin, J. K. Suppression of extracellular signals and cell proliferation through EGF receptor binding by (−)-epigallocatechin gallate in human A431 epidermoid carcinoma cells. J. Cell. Biochem., *67:* 55–65, 1997.

16. Dong, Z. Effects of food factors on signal transduction pathways. Biofactors, *12:* 17–28, 2000.

17. Yang, F., Oz, H. S., Barve, S., de Villiers, W. J., McClain, C. J., and Varilek, G. W. The green tea polyphenol (-)-epigallocatechin-3-gallate blocks nuclear factor-κB activation by inhibiting IκB kinase activity in the intestinal epithelial cell line IEC-6. Mol. Pharmacol., *60:* 528–533, 2001.

18. Kim, J., Hwang, J. S., Cho, Y. K., Han, Y., Jeon, Y. J., and Yang, K. H. Protective effects of (−)-epigallocatechin-3-gallate on UVA- and UVB-induced skin damage. Skin Pharmacol. Appl. Skin Physiol., *14:* 11–19, 2001.

19. Yang, F., de Villiers, W. J., McClain, C. J., and Varilek, G. W. Green tea polyphenols block endotoxin-induced tumor necrosis factor production and lethality in a murine model. J. Nutr., *128:* 2334–2340, 1998.

20. Romieu-Mourez, R., Landesman-Bollag, E., Seldin, D. C., Traish, A. M., Mercurio, F., and Sonenshein, G. E. Roles of IKK kinases and protein kinase CK2 in activation of nuclear factor-κB in breast cancer. Cancer Res., *61:* 3810–3818, 2001.